THE ROLES OF Mcl-1 AND Bcl-x IN CENTRAL NERVOUS SYSTEM DEVELOPMENT

by

© Lauren Caroline Fogarty

A Thesis submitted to the

School of Graduate Studies

in partial fulfilment of the requirements for the degree of

Master of Science in Medicine (Neuroscience)

Division of BioMedical Sciences/Faculty of Medicine

Memorial University of Newfoundland

October 2015

St. John's Newfoundland and Labrador

Abstract

Changes in survival signaling through the stages of developmental neurogenesis are poorly understood. This thesis examined the role of anti-apoptotic Bcl-2 proteins, Mcl-1 and Bcl-x in promoting survival as cells progress through neurogenesis using Nestin-mediated conditional deletion of *mcl-1*, *bcl-x* or both in the mouse embryonic central nervous system. My results show Mcl-1 is required earlier in development in precursor populations, while Bcl-x is required for the post-mitotic cells. However, loss of a single *bcl-x* allele exasperated apoptotic death in the *mcl-1* knockout revealing a novel role for Bcl-x in precursor cells. Furthermore, the double knockout exhibited a more severe phenotype with complete loss of the central nervous system. To determine how Mcl-1 and Bcl-x promote cell survival, qPCR and *in situ* hybridization were used to examine the expression profiles of pro-apoptotic *bcl-2* genes. This study demonstrates the distinct and overlapping requirements of Mcl-1 and Bcl-x through murine neural development.

Acknowledgements

I would first and foremost like to thank my supervisor Dr. Jackie Vanderluit for her guidance, patience and support throughout the completion of this thesis. Without her direction and assistance I would not have been able to complete this project.

I would also like to thank my supervisory committee members Dr. Xihua Chen and Dr. Michiru Hirasawa for their insightful comments and assistance with the preparation of this thesis.

Collaborators Dr. Maria Licursi and Dr. Kensuke Hirasawa are thanked for their assistance in completeing qPCR experiments.

Finally, thank you to my lab members, friends and family for their help and support throughout this program.

List of Abbreviations

µg - Microgram

µl – Microliter

°C – Degrees Celsius

A – Anterior

A1 - Bcl-2-related protein A1

AC3 - Active caspase-3

Apaf-1 - Apoptotic protease activation factor-1

B - Basal

Bad - Bcl-2 antagonist of cell death

BCIP – 5-bromo-4-chloro-3-indolyl-phosphate

Bcl-xl - Bcl-2-related gene long isoform

BH - Bcl-2 homology

Bid - Bcl-2-interacting domain death agonist

Bik - BH3 interacting killer

Bim - Bcl-2 interacting mediator of cell death

BKO - Bcl-x conditional knockout

Bmf - Bcl-2 modifying factor

Bp – Base pair

BrdU - Bromodeoxyuridine

CNS - Central nervous system

CP - Cortical plate

CT - Threshold cycle

Ctl - Control

CV - Cresyl violet

D - Dorsal

dd H_2O – Double-distilled water

DEPC – Diethyl pyrocarbonate

DIG - Digoxigenin

DKO - Double knockout

DMSO – Dimethyl sulfoxide

dNTP – Deoxynucleotide triphosphate

DTT - Dithiothreitol

E - Embryonic Day

EDTA – Ethylenediaminetetraacetic acid

FMN - Facial motor nucleus

Het - Heterozygote

Hrk - Harakiri Bcl-2 interacting protein

IP - Immunoprecipitation

IPC - Intermediate progenitor cells

IZ - Intermediate zone

KO - Knockout

L – Lateral

M – Medial

MABT – Maleic acid

mM – Millimolar

MCl-1 - Myeloid cell leukemia-1

MKO - Mcl-1 conditional knockout

MOMP - Mitochondrial outer membrane permeabilization

MZ - Marginal zone

NBT – 4-Nitroblue tetrazolium

ORG - Outer radial glia

P – Posterior

PBS - Phosphate buffered saline

PCR - Polymerase chain reaction

PFA - Paraformaldehyde

PMSF - Phenylmethylsulfonyl fluoride

PUMA - p53 upregulated modulator of apoptosis

qRT-PCR - Quantitative real time polymerase chain reaction

RG - Radial glia

RQ - Relative quantity

SDS - Sodium dodecyl sulfate

SVZ - Subventricular zone

TE - Tris-Ethylenediaminetetraacetic acid

TPBS - Tween-20 phosphate buffered saline

V – Ventral

VZ - Ventricular zone

Table of Contents

List of Tables

List of Figures

1.0 Introduction

1.1 Overview

During development, neuronal numbers are regulated by a balance between proliferation and programmed cell death. Apoptosis is a form of programmed cell death that plays a critical role in normal development of many systems within the body. Specifically within central nervous system (CNS) development, apoptosis eliminates unnecessary connections and allows for morphological changes (e.g. the formation of digits). In humans, disregulation of apoptosis in the CNS occurs in a number of developmental as well as adult neuropathological disorders including stroke, Parkinson's disease, Alzheimer's disease and ALS (Chen, Curran & Morgan 1995). The B-cell lymphoma 2 (Bcl-2) proteins are one of the key families of proteins that regulate the initiation of apoptotic death pathways. The human Bcl-2 family is conserved within rodents, making them an excellent model for studying Bcl-2 protein requirements. Currently there is little understanding of which Bcl-2 family members are necessary to maintain the balance between cell death and survival throughout CNS development.

1.2 Neurogenesis

Neural development is a strictly regulated process. Of the 21-day gestation period of mice, neurulation begins by embryonic day 7.5 (E7.5) (Krajewska et al.

2002). First, the primitive neural tube is formed from a thickening in the ectodermal germ layer termed the neural plate (Krajewska et al. 2002). More specifically, the neural plate is composed of neural epithelial cells, which are the primitive neural stem cells. Invagination along the midline of the neural plate and closure of the dorsal aspects of the neural fold form the completed neural tube by approximately E10 (Allen Brain Atlas, 2012). At this time there is a great deal of proliferation that occurs along the neural tube, forming enlarged subspecified regions of the CNS. E10 is also when the earliest neurogenesis begins within the CNS (Nornes & Carry 1978; Sims & Vaughn 1979; McConnell 1981). Folding of the neural tube at the rostral end initially forms three brain vesicles, the developing forebrain, midbrain and hindbrain. As development progresses additional brain vesicles are formed giving further specification to individual brain regions until the five vesicle stage, at which point the basic plan of the nervous system has formed (Jessell 2000). Early development of the CNS establishes a pool of progenitor cells prior to the onset of differentiation and neurogenesis.

Neurogenesis begins in the murine nervous system at approximately E10 in the spinal cord and hindbrain, but later at E11 within the cortex and is terminated by E17 (Angevine & Sidman 1961; Nornes & Carry 1978). Post-mitotic neurons are formed either directly from the primitive neural stems cells, the neural epithelial cells, or from further fate restricted neural progenitor cells (Molnár 2011). Neural epithelial cells form the most apical layer of the early CNS, the ventricular zone (VZ).

Prior to the onset of neurogenesis, the neural epithelial cells divide symmetrically producing two identical daughter cells therefore expanding the pool of stem cells (Haubensak et al. 2004; Götz & Huttner 2005). Initial expansion of the precursor pool followed by timed differentiation beginning at E10 leads to the formation and development of specified regions of the CNS.

1.2.1 Spinal Cord Neurogenesis

The ventral spinal cord contains populations of cells transmitting motor function, while the dorsal aspect relays sensory information from the periphery up the spinal cord to the brain (Caspary & Anderson 2003). Cell type fate in the spinal cord is determined early in development based on the expression of neuron-specific markers along the dorsoventral axis (Caspary & Anderson 2003). The mature murine spinal cord contains 5 distinguishable laminae in the dorsal aspect, which are a result of orchestrated cell migration and arrangement (Jessell 2000). By E9.5 neural progenitor cells line the VZ and express molecular markers specific to their dorsoventral position (Jessell 2000; Briscoe & Ericson 2001). It is at this time that neurogenesis begins in the spinal cord (Nornes & Carry 1978). Progenitor cells along the midline begin to differentiate and migrate to the mantle layer (Figure 1.1B) where they express further cell type specific markers (Caspary & Anderson 2003). From the mantle layer cells will migrate to their final position within the spinal cord, which is determined by the initial location of the cell along the midline

dorsoventral axis and their time of their birth (Caspary & Anderson 2003). In general, cells born along the dorsal portion of the VZ will migrate to reside in the dorsal spinal cord (Caspary & Anderson 2003). However, later born cells tend to have a reversed final position along the dorsoventral axis (Caspary & Anderson 2003). Neurogenesis progresses in general in a ventral-dorsal pattern within the developing spinal cord, with the earliest neurogenesis occurring in the ventral populations (McConnell 1981; Caspary & Anderson 2003). Dorsoventral position as well as time of birth regulates the neural type and final position of neurons throughout the spinal cord.

Figure 1.1: Regions of the developing CNS and spinal cord.

(A) Diagram of a sagittal section from an E11 whole embryo. Colours indicate various developing CNS structures. Box indicates region of spinal cord shown in B. (B) Diagram of a coronal section of E11 spinal cord indicating general cell populations during spinal cord development. A= anterior, P= posterior.

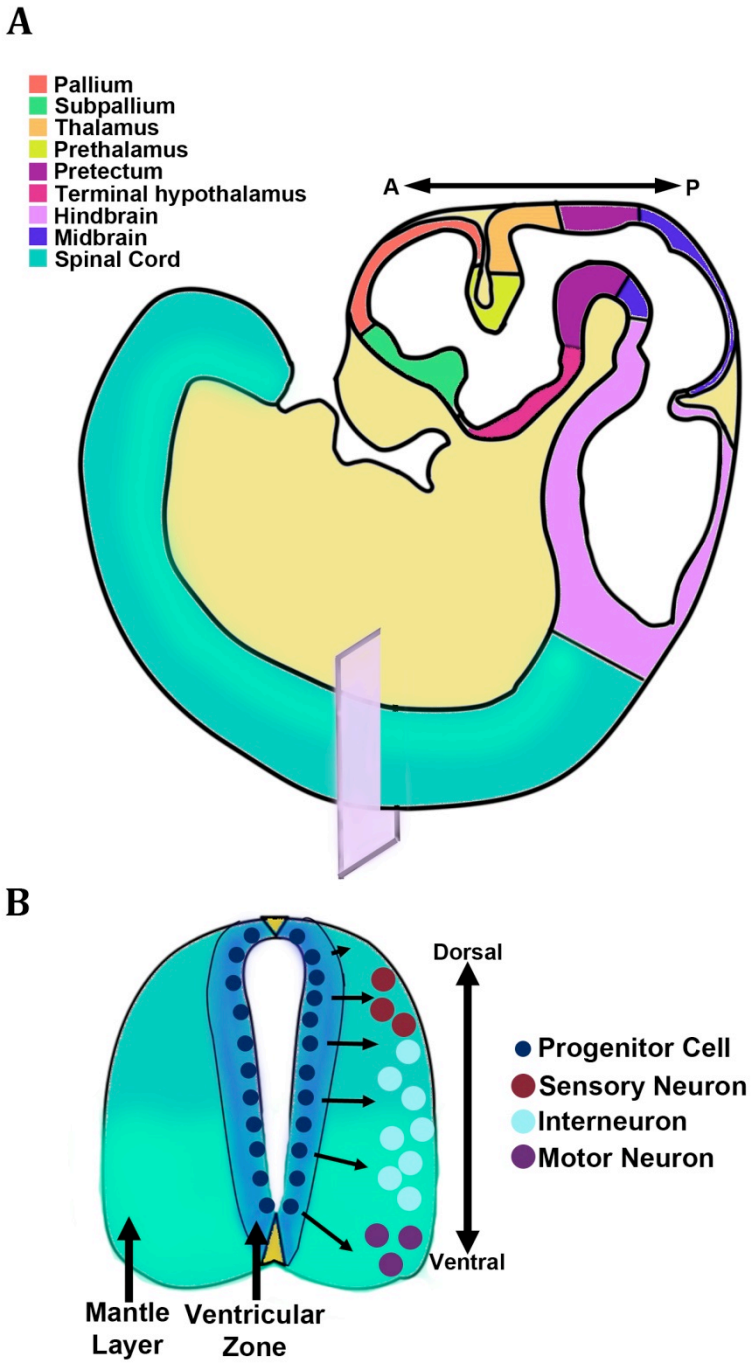
A
Pallium
Subpallium
Thalamus
Prethalamus
Pretectum
Terminal hypothalamus
Hindbrain
Midbrain
Spinal Cord
A
P
B
Dorsal
Ventral
Progenitor Cell
Sensory Neuron
Interneuron
Motor Neuron
Mantle Layer
Ventricular Zone

1.2.2 Forebrain Neurogenesis

By E10 within the cortex, neural epithelial cells begin to differentiate to form radial glial cells. These cells are the primary stem cell found in the further developed VZ and largely replace the neural epithelial population (Metcalfe et al. 2004). Like neural epithelial cells, radial glial cells are bipolar and extend from the apical surface and send a projection to the basal surface (Fietz & Huttner 2011). Inner radial glial cells divide symmetrically to self-renew and maintain their population, or differentiate to generate further restricted progenitor cells of the subventricular zone (SVZ) or post-mitotic neurons (Molnár 2011). Intermediate progenitor cells and outer radial glial cells are both progeny of the inner radial glial cells and differentiate to produce post-mitotic neurons (Figure 1.2). Like the inner radial glial cells, outer radial glial cells have an extended process that travels to the basal surface although they are also distinct from the inner radial glial cells as their cell bodies reside in the SVZ and they do not have an extended process traveling to the apical surface (Molnár 2011). Intermediate progenitor cells give rise to differentiating neuroblasts that migrate away from the apical surface to form the cortical layers of post-mitotic neurons (Molnár 2011). Cortical neurogensis begins slightly later in development than other regions of the CNS and also forms the layers of the cortex in an inside-out manner.

Figure 1.2: Cellular layers of cortical development.

The progenitors in the developing murine cortex include inner radial glia (IRG), outer radial glia (ORG) and intermediate progenitor cells (IPC). These progenitors are all capable of proliferating to maintain their populations as well as differentiating to form the post-mitotic neurons of the cortical plate. (Adapted from Molnár et al. 2011).

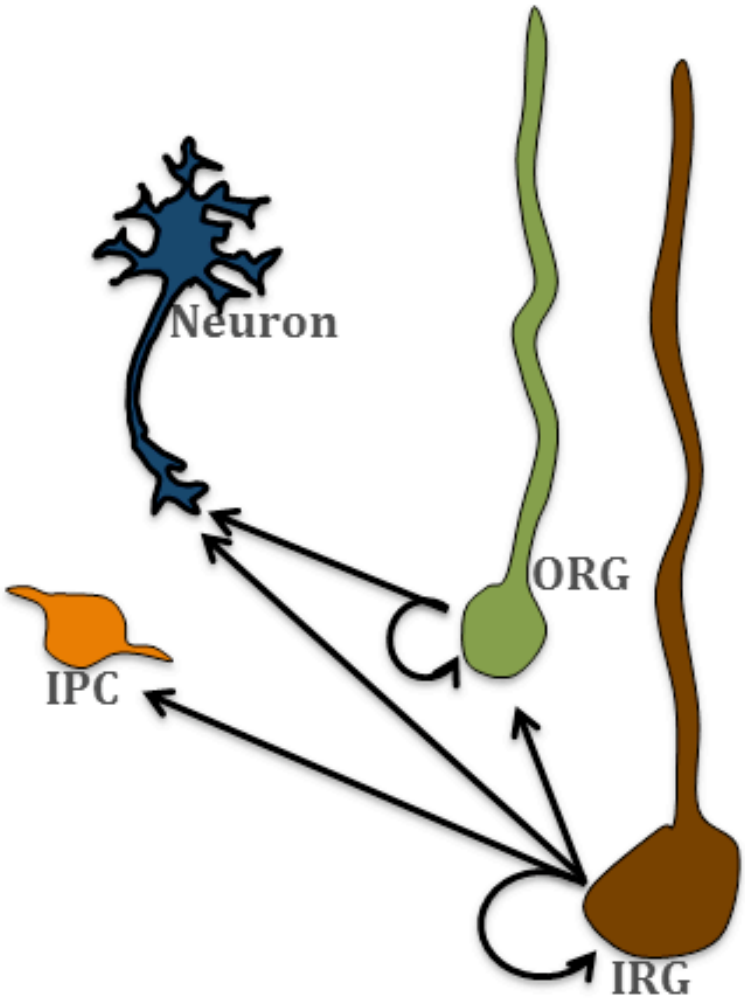
Neuron
ORG
IPC
IRG

1.3 Developmental Apoptosis

Apoptosis is a strictly regulated form of cell death allowing cells to be broken down in a programmed and contained manner, most commonly occurring through the mitochondrial pathway (Hotchkiss et al. 2009). Apoptosis is critical in maintaining healthy tissues offering an isolated form of cell death in the case of cellular damage. It is also essential in the development of tissues. Specifically in nervous system development, apoptosis occurs in neurons, glia as well as progenitor cells (Nijhawan et al. 2000; Kristiansen & Ham 2014). It is estimated that as much as 50% of the original cell population is lost during nervous system development resulting in optimal synaptic connections and pattern formation (Oppenheim 1981). Throughout both embryonic and post-natal neural development, significant apoptosis occurs in the rodent CNS (White & Barone 2001). Apoptotic cells are cleared within several hours and therefore at any given time only 2-3% of cells in a region are undergoing apotosis (Bursch et al. 1990; White & Barone 2001). It is well established that apoptosis is critical for the maintenance of proper neuronal numbers, elimination of neurons that do not reach synaptic targets and formation of morphological features of the nervous system (Oppenheim 1991). The controlled process of apoptosis allows for the removal of damaged or unnecessary cells in a contained manner without triggering immune responses or disruption to neighboring cells.

1.4 Apoptosis

The term apoptosis was first used in 1972 when describing an intrinsic cell suicide program (Kerr et al. 1972). Apoptosis regulates development through morphological changes as well as eliminates unnecessary connections within the CNS. It may be initiated through the extrinsic or intrinsic pathways. Ultimately, these pathways converge to induce mitochondrial outer membrane permeabilization and the activation of cellular mechanisms to degrade the cellular components (Figure 1.3). Characteristic morphological features of cells undergoing apoptosis include condensation of cellular components, chromatin condensation, DNA fragmentation, nuclear fragmentation and formation of membrane bound apoptotic bodies (Nijhawan et al. 2000). A number of proteins and proteins families regulate apoptosis, including the Bcl-2 family, the inhibitors of apoptosis (IAP), the caspases, Smac/DIABLO, cytochrome c and Apaf-1 (Green 2000). However, the two major regulatory protein families are the Caspases and the Bcl-2 family proteins.

Figure 1.3: The intrinsic apoptotic pathway.

The Bcl-2 family proteins (BH3-only, anti-apoptotic, and effectors) regulate mitochondrial membrane permeabilization. Once the effector proteins are activated and insert into the outer mitochondrial membrane, cytochrome c is released into the cytosol. This triggers the assembly of the apoptosome and the caspase cascade (active caspase-3), which proceeds to degrade the cellular components resulting in apoptosis. (Adapted from Youle & Strasser, 2008.)

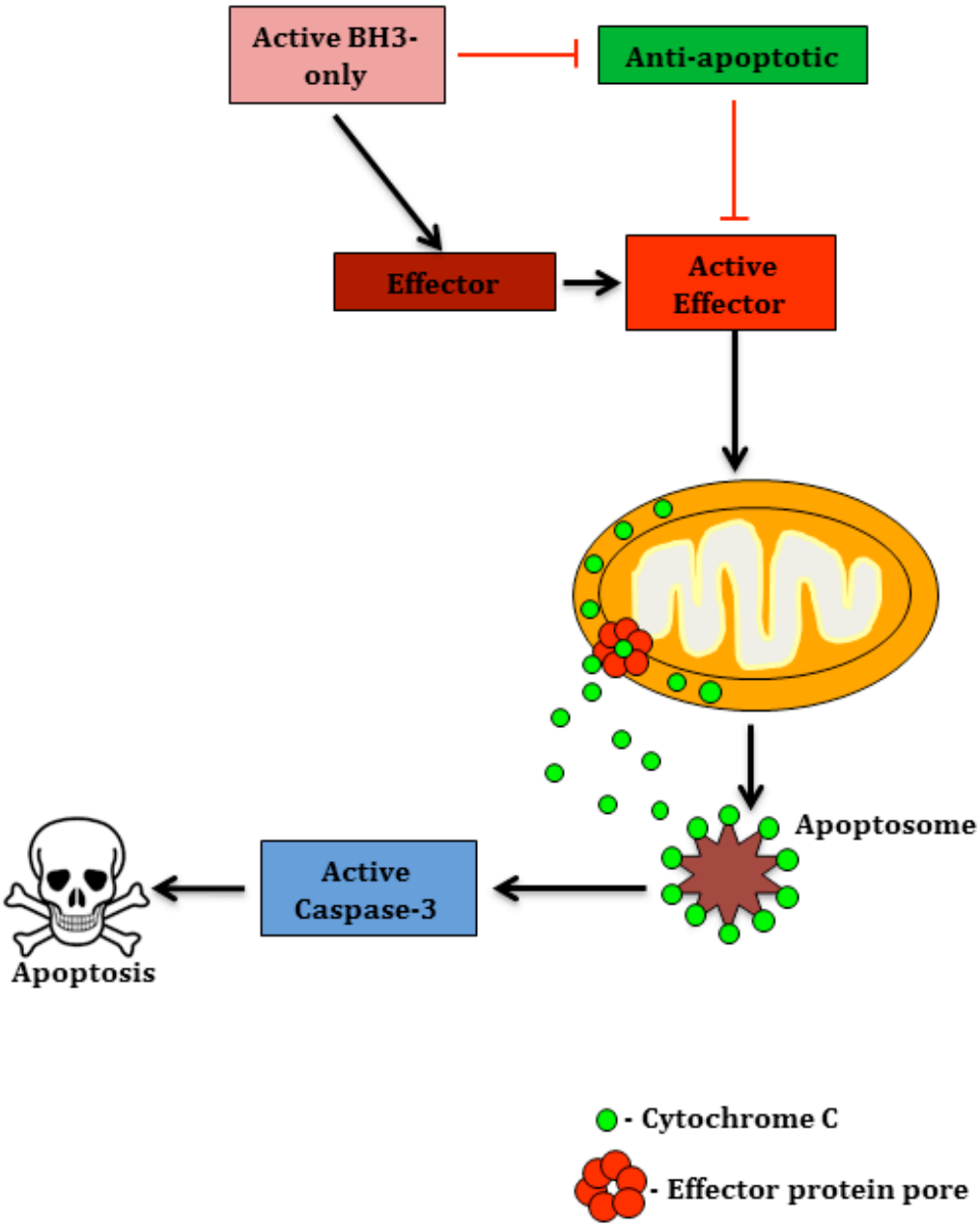
Active BH3-only
Anti-apoptotic
Effector
Active Effector
Apoptosome
Active Caspase-3
Apoptosis
- Cytochrome C
- Effector protein pore

1.5 The Caspases

The cysteine-aspartic acid proteases are members of the interleukin-1β-converting enzyme family sharing common properties including a conserved pentapeptide active site 'QACXG' where X can be R, Q or D (Fan et al. 2005). There have been 14 caspases identified thus far; all contain a highly diverse N-terminal structure required for the activation of their precursor form known as procaspases (Fan et al. 2005). Once activated, either by other caspases or self-activation, the caspases form dimers, which will then form the enzymatically active tetramers (Fan et al. 2005).

The caspases may be broken down into three groups based on their sequence homology (Table 1.1), with subfamilies I and II involved in the activation and execution of apoptosis (Fan et al. 2005). Subfamily I is comprised of the initiator caspases. They are activated by death signaling and propagate the apoptotic signal (Thornberry & Lazebnik 1998). Subfamily II contains the apoptosis executioner caspases. Once activated, these caspases degrade the cellular components (Savill & Fadok 2000). Caspase activation will ultimately lead to the destruction of the cellular components and cell death.

Table 1.1:Classification of the caspase family.

Subfamily	Caspase	Function
Group 1	Caspase-2	Initiator Caspase
	Caspase-8	Initiator Caspase
	Caspase-9	Initiator Caspase
	Caspase-10	Initiator Caspase
Group 2	Caspase-3	Effector Caspase
	Caspase-6	Effector Caspase
	Caspase-7	Effector Caspase
Group 3	Caspase-1	Inflammatory Caspase
	Caspase-4	Inflammatory Caspase
	Caspase-5	Inflammatory Caspase
	Caspase-12	Inflammatory Caspase
	Caspase-13	Inflammatory Caspase
	Caspase-14	Inflammatory Caspase

The caspases are integral to the induction, transduction and amplification of intracellular apoptotic signaling. There are two pathways capable of inducing caspase activation: the extrinsic and the intrinsic apoptotic pathways. The extrinsic pathway is a death receptor-mediated pathway initiated by the ligation of cell death receptors such as Fas and tumor necrosis factor receptor-1 and proceeds independent of the Bcl-2 family proteins (Youle & Strasser 2008). Bcl-2 family proteins are upstream regulators of mitochondrial permeabilization required for the intrinsic apoptotic pathway. The intrinsic or mitochondrion-mediated pathway is initiated by cellular stress such as DNA damage leading to outer mitochondrial membrane permeabilization resulting from Bcl-2 family protein activation. This

results in the release of cytochrome c into the cytoplasm, where in the presence of ATP, the apoptotic protease activation factor-1 (Apaf-1) oligomerizes forming the apoptosome together with initiator procaspase-9 (Fan et al. 2005). The cleavage and activation of caspase-9 begins a cascade of executioner caspase activation causing degradation of cellular components as well as a positive feedback loop activating more procaspase-9 and amplifying the signal (Fan et al. 2005). This cascade includes the cleavage of caspase 3, a common marker of apoptosis. The activation of caspase 3 is considered to be a point of no return in the apoptotic pathway and with the presence of a condense nucleus is regarded as a reliable indicator of apoptotic cell death (Boatright & Salvesen 2003). The caspases are responsible for the amplification of the apoptotic signal as well as the degradation of cellular components, but it is the Bcl-2 family proteins that regulate the initiation of the caspase cascade.

1.6 Bcl-2 Family Proteins

The release of cytochrome c is a significant regulatory step in the apoptotic pathway as it results in the activation of the caspase cascade and signifies the point of no return for the cell (Nijhawan et al. 2000). The release of cytochrome c is regulated by the Bcl-2 family proteins acting in response to developmental cues or cytotoxic insults (Czabotar et al. 2014). Vaux, Cory and Adams (1988) first described the molecular role of the Bcl-2 family proteins in apoptosis when they showed elevated expression of Bcl-2 in follicular lymphoma influenced the apoptotic

response. This study helped to elucidate the molecular pathways that regulate apoptosis.

The Bcl-2 family is composed of both anti-apoptotic and pro-apoptotic proteins that interact and regulate one another's actions to initiate the intrinsic apoptotic pathway. Bcl-2 family proteins are structurally related, each containing one to four alpha helical Bcl-2 homology (BH) domains (Youle & Strasser 2008). These BH domains allow for their binding with one another and define their pro-survival or pro-apoptotic properties (Youle & Strasser 2008). Bcl-2 family proteins are further subdivided into three groups based on their structural similarities as well as function: anti-apoptotic proteins, BH3-only proteins and the pro-apoptotic effector proteins (Figure 1.4). These three groups of Bcl-2 proteins are capable of interacting with and inhibiting each other's actions.

The pro-apoptotic effector proteins of the Bcl-2 family include Bcl-2 antagonistic killer 1 (Bak) and Bcl-2-associated X protein (Bax). Both are critical to the outer mitochondrial membrane permeability. These effectors contain BH1, BH2, BH3 and BH4 domains and when in their active conformation, are capable of oligomerizing and inserting into the outer mitochondrial membrane leading to its permeabilization (Czabotar et al., 2014). It is thought their function and activation are strictly regulated by other Bcl-2 family members (Czabotar et al., 2014). Both Bax and Bak are constitutively expressed and have been shown to be present at the outer mitochondrial membrane in their inactive confirmation or bound by other Bcl-2 proteins inhibiting their activity (Schellenberg et al. 2013; Peng et al. 2013;

Vela et al. 2013). In a healthy cell, the pro-apoptotic effector proteins cycle from the cytosol to the outer mitochondrial membrane and back without initiating apoptosis (Schellenberg et al. 2013).

Figure 1.4: Members of the *bcl-2* family.

Anti-apoptotic and pro-apoptotic members of the *bcl-2* family genes outlining conserved BH domains. BH3-only pro-apoptotic family members are further divided into BH3-only activators and sensitizers. (Adapted from Youle & Strasser, 2008)

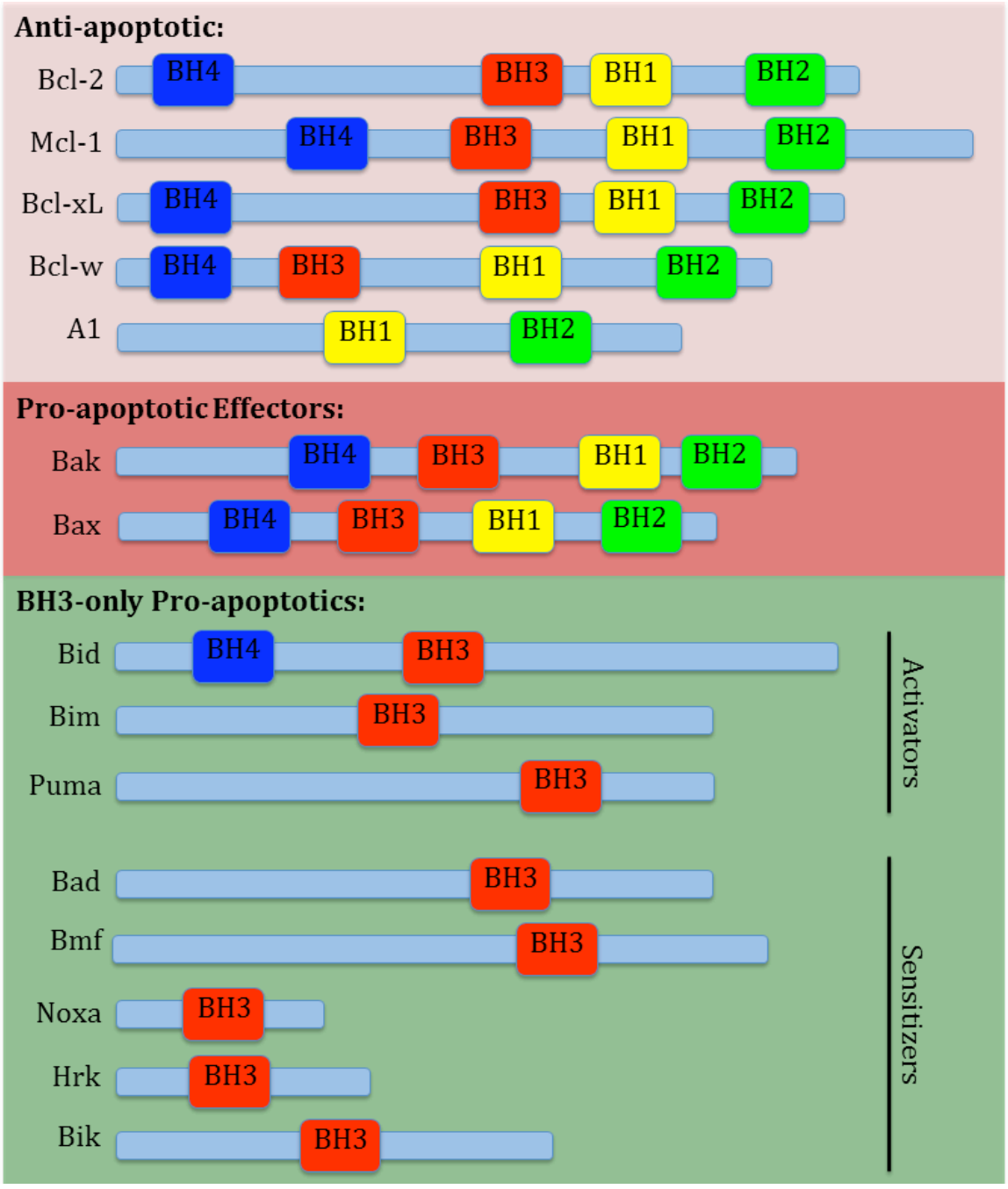
Anti-apoptotic:
Bcl-2
BH4
BH3
BH1
BH2
Mcl-1
BH4
BH3
BH1
BH2
Bcl-xL
BH4
BH3
BH1
BH2
Bcl-w
BH4
BH3
BH1
BH2
A1
BH1
BH2
Pro-apoptotic Effectors:
Bak
BH4
BH3
BH1
BH2
Bax
BH4
BH3
BH1
BH2
BH3-only Pro-apoptotics:
Bid
BH4
BH3
Bim
BH3
Puma
BH3
Activators
Bad
BH3
Bmf
BH3
Noxa
BH3
Hrk
BH3
Bik
BH3
Sensitizers

The second group of pro-apoptotic proteins in the Bcl-2 family, the BH3-only pro-apoptotics, includes Bcl-2-interacting domain death agonist (Bid), Bcl-2 interacting mediator of cell death (Bim), p53 upregulated modulator of apoptosis (Puma), Bcl-2 antagonist of cell death (Bad), Bcl-2 modifying factor (Bmf), Noxa, harakiri Bcl-2 interacting protein (Hrk), and BH3 interacting killer (Bik) (Figure 1.4). As their classification would suggest, the only structural similarity of the BH3-only proteins is the BH3 domain, which they require for their targeted binding (Lomonosova & Chinnadurai 2008). The BH3-only proteins act as sensors in the system and are activated or transcriptionally upregulated in response to apoptotic stimuli from various cellular processes (Ola et al. 2011). It is thought the BH3-only proteins can act as direct activators of the effector proteins promoting their homo-oligomerization and outer mitochondrial membrane permeabilisation (Shamas-Din et al. 2013). Alternatively, the BH3-only proteins may also promote apoptosis by binding and occupying the anti-apoptotic Bcl-2 proteins (Shamas-Din et al. 2013). The binding properties of these proteins have been extensively studied, however the exact mechanisms of action and regulation of other Bcl-2 family proteins is still debated.

The anti-apoptotic Bcl-2 proteins include Bcl-2, myeloid cell leukemia-1 (Mcl-1), Bcl-2-related gene long isoform (Bcl-xl), Bcl-w and Bcl-2-related protein A1 (A1). With the exception of A1, the anti-apoptotic proteins contain all four BH domains and selectively bind and inhibit the activity of both the effector and BH3-

only pro-apoptotic family members (Ola et al. 2011; Youle & Strasser 2008). Therefore, the control of anti-apoptotic protein concentration in part allows cells to control their fate. Bcl-xl for example, is upregulated transcriptionally in response to growth factors (Grad et al. 2000). Mcl-1, another anti-apoptotic family member is quickly degraded within the cell through ubiquitination and proteasomal degradation (Zhong et al. 2005), but can also be upregulated post-transcriptionally by slowing the rate of degradation (Zhong et al. 2005; Cuconati & Mukherjee 2003). Regulating anti-apoptotic protein expression is one of the methods cells use to control their fate. The ratio of anti-apoptotic to pro-apoptotic Bcl-2 proteins within a cell has been shown to determine its susceptibility to either resisting or undergoing apoptosis (Ola et al. 2011). While the concentration of anti-apoptotic proteins does affect cell survival, the binding specificity of those expressed is also a factor.

There is a great deal of redundancy in the binding capabilities of the Bcl-2 family proteins. However, there is also preferential binding specificity amongst anti- and pro-apoptotic family members (Dutta et al. 2010). It has been shown that Bim, Bid, Puma, Bik and Bmf bind all 5 anti-apoptotic proteins (Figure 1.5), however, Bad preferentially binds Bcl-2, Bcl-xl and Bcl-w while Noxa has a greater affinity for Mcl-1 and A1 (Chen et al., 2005; Czabotar et al., 2014; Letai et al., 2002). Furthermore, it is currently thought the effector protein Bak has a greater binding affinity for Bcl-xL and Mcl-1 while Bax shows equal binding capabilities for all of the anti-apoptotic

proteins (Czabotar et al., 2014). Numerous studies have been completed examining the binding capabilities among family members and though a great deal is understood of their quaternary structure, there are still a number of inconsistencies in the literature (Chen et al. 2005; Letai et al. 2002). Bax binding with Mcl-1 is disputed as well as the binding of Hrk and Bad with Bcl-xL (Chen et al. 2005; Chipuk et al. 2010; Letai et al. 2002; Moldoveanu et al. 2014). Despite these inconsistencies it is well accepted that numerous redundancies in binding exist within the Bcl-2 family. A similarity in binding capabilities of Bcl-2 family members also suggests redundancy of their function. While the binding affinities of the proteins have mostly been elucidated, the exact mechanism of how the Bcl-2 family proteins interact and regulate each other's activities is still under investigation.

Figure 1.5: Binding affinities of Bcl-2 family proteins.

Binding capabilities of the pro-apoptotic Bcl-2 family proteins with Mcl-1 and Bcl-x. Red indicates effectors, pink indicates direct activators, yellow indicates sensitizers and green indicates anti-apoptotic Bcl-2 family proteins. Underlined proteins have unique binding preferences for either Mcl-1 or Bcl-xL. (Adapted from Moldoveanu et al. 2014).

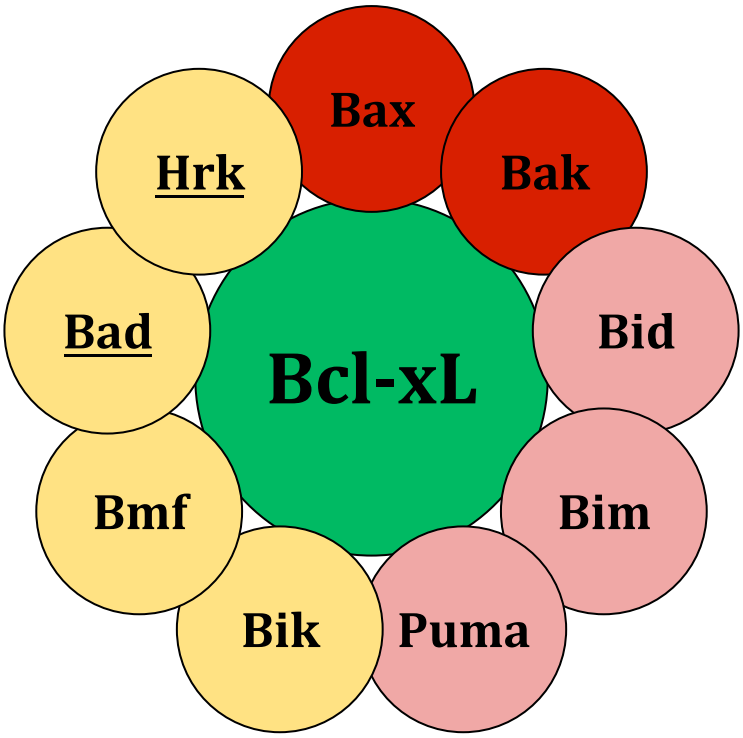
Bax
Hrk
Bak
Bad
Bcl-xL
Bid
Bmf
Bim
Bik
Puma

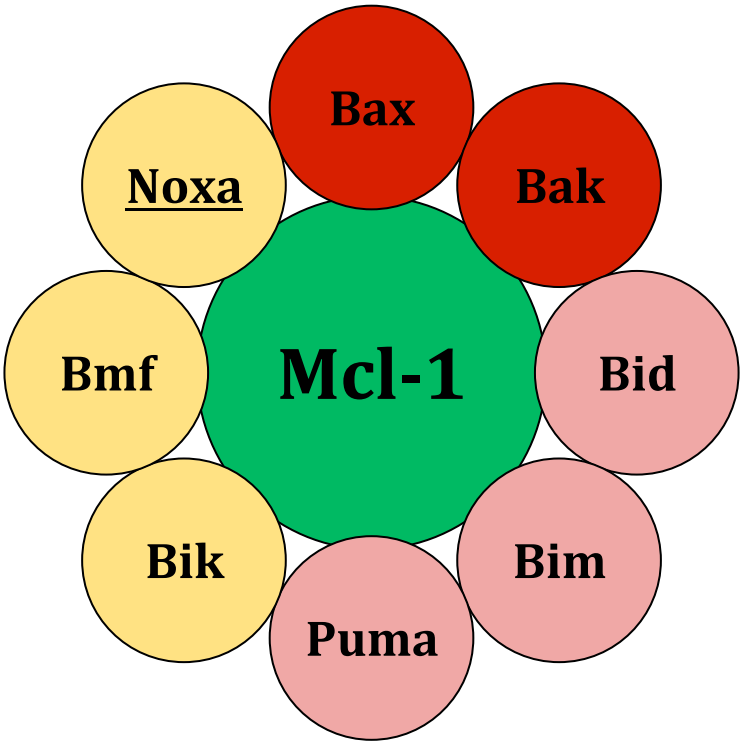
Bax
Noxa
Bak
Bmf
Mcl-1
Bid
Bik
Bim
Puma

1.7 Models of interaction amongst the Bcl-2 family

When considering the role of any individual Bcl-2 family member, their mechanism of action must also be understood. Currently there are a number of theories regarding the mechanisms of Bcl-2 family protein regulation of the outer mitochondrial membrane integrity. Three of the most widely accepted models of Bcl-2 family interaction include the indirect activation model, the direct activation model and the unified model (Figure 1.6). The neutralization or indirect activation model proposes that the effector proteins (Bax and Bak) are spontaneously activated and thus inhibition of anti-apoptotic family members by the BH3-only proteins is sufficient to induce outer mitochondrial membrane permeabilization (Willis et al. 2007; Willis et al. 2005; Uren et al. 2007). Alternatively, the direct-activation model stipulates that the BH3-only proteins are further subdivided into sensitizers/depressors as well as direct activators (Letai et al. 2002; Kuwana et al. 2002; Kuwana et al. 2005; Wei et al. 2000). The role of the sensitizer/depressor proteins is to inhibit the anti-apoptotic proteins, while the direct activator proteins activate Bax and Bak initiating their oligomerization and pore formation in the mitochondrial membrane (Kuwana et al. 2002; Kuwana et al. 2005; Letai et al. 2002; Wei et al. 2000). A third commonly accepted theory is the unified model. The unified model combines aspects of both the direct and indirect activation models, suggesting that there are two modes of inhibition of mitochondrial permeabilization (Llambi et al. 2011). It states that anti-apoptotic proteins are capable of

sequestering both the BH3-only proteins as well as activated Bax or Bak through the two modes of inhibition (Llambi et al. 2011). Anti-apoptotic Bcl-2 proteins therefore, act at two steps in the apoptotic pathway to inhibit the BH3-only proteins at the initiation stage and inhibit the Bcl-2 effector proteins at the mitochondria.

Figure 1.6: Mechanisms of regulation of the Bcl-2 proteins.

Three leading models of the mechanism of regulation of Bcl-2 family proteins. **(A)** Direct activation model requires BH3-only proteins (pink) to activate the effectors Bax/Bak (red). **(B)** Indirect activation model proposes the effector proteins are constitutively activated, but may be inhibited by anti-apoptotic Bcl-2 proteins (green). **(C)** The unified model combines theories of both the direct and indirect models suggesting there are two modes of regulation. (Adapted from Czabotar et al., 2014.)

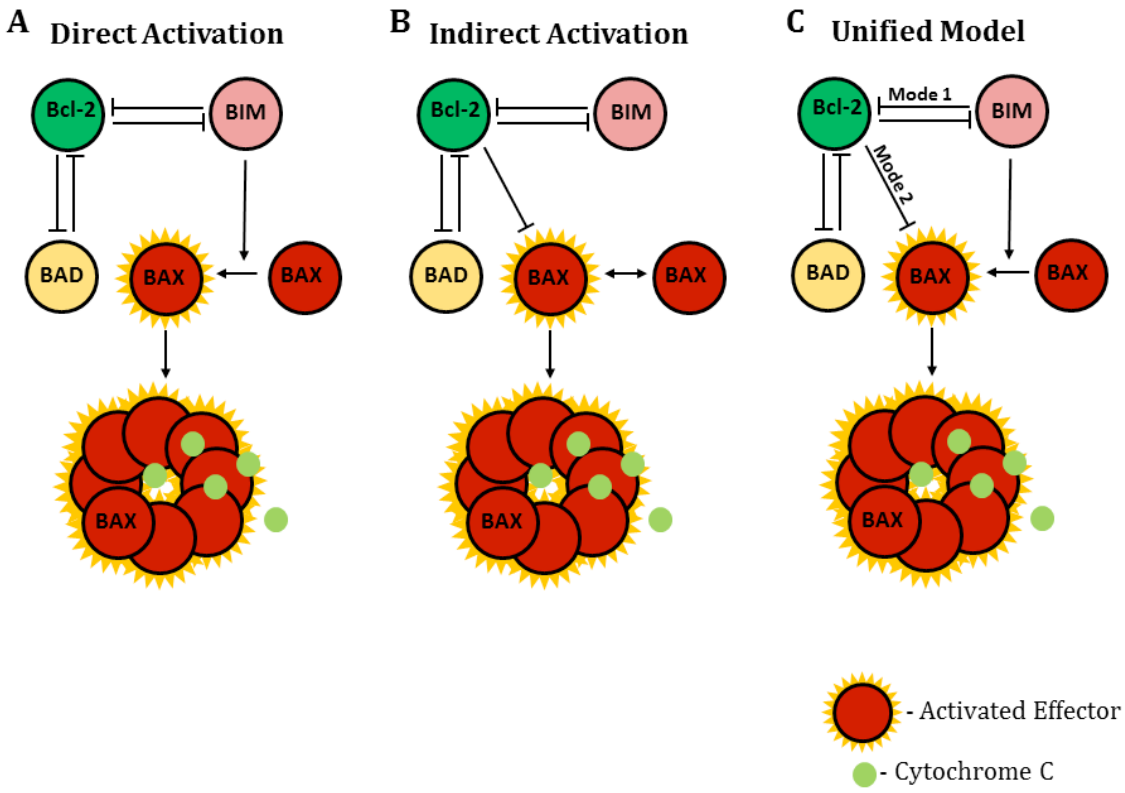
A
Direct Activation
Bcl-2
BIM
BAD
BAX
BAX
BAX
B
Indirect Activation
Bcl-2
BIM
BAD
BAX
BAX
BAX
C
Unified Model
Mode 1
Mode 2
Bcl-2
BIM
BAD
BAX
BAX
BAX
- Activated Effector
- Cytochrome C

1.8 Mcl-1

The role of anti-apoptotic Bcl-2 family proteins in CNS development has been studied to a limited extent. Previous knockdown and knockout studies have demonstrated the loss of A1, Bcl-w or Bcl-2 have no apparent effects on the development of the CNS (Michaelidis et al. 1996; Hamasaki et al. 1998; Print et al. 1998; Ross et al. 1998). The disruption of Mcl-1 or Bcl-x, however, does have significant impacts on proper CNS development (Arbour et al. 2008; Motoyama et al. 1995; Rinkenberger et al. 2000; Roth et al. 1996). *mcl-1* was first discovered as a unique gene upregulated during the differentiation of human myeloid leukemia cells (Kozopas et al. 1993). Though it has been shown to play a role in the regulation of neural precursor cell terminal differentiation (Hasan et al. 2013), Mcl-1 is primarily known for its regulation of apoptosis.

As a widely expressed anti-apoptotic Bcl-2 family member, Mcl-1 is critical during mammalian development. In *mcl-1* germline deletion, embryonic lethality occurs very early in development (E3.5) due to defects in trophectoderm differentiation (Rinkenberger et al. 2000). This demonstrates a developmental requirement for Mcl-1 but also provides challenges for loss-of-function studies at later developmental time points. To overcome this early lethality, a number of tissue-specific conditional knockout models have been created to study the

requirement for Mcl-1 at later time points and in different tissue types throughout development as well as in adults.

To investigate the cell survival requirements of Mcl-1, many studies have utilized conditional knockout models specific to various tissue types including hematopoietic stem cells (Opferman et al. 2005), lymphoid development (Dzhagalov, Dunkle, & He, 2008; Opferman et al., 2003; Vikstrom et al., 2010), neutrophils (Dzhagalov, John, & He, 2007; Steimer et al., 2009), cardiomyocytes (Wang et al. 2013) as well as neurons (Arbour et al. 2008; Malone et al. 2012). The Cre-Lox system (Sauer 1998) is one method that has been used to selectively knockdown *mcl-1* gene expression. With this method, the genes of interest are flanked by loxP sites that are recognized and cleaved by Cre recombinase efficiently excising the gene. The expression of Cre recombinase is driven by a tissue specific promoter, restricting gene deletion to the chosen cell populations. The Cre-Lox system provides advantages over germline knockouts allowing for a specific population to be targeted. Additionally, the timing of the gene deletion is selective depending on the promoter used. Within the CNS, two *mcl-1* Cre-Lox conditional knockout mice have been designed using Foxg1 and Nestin promoters causing a loss of Mcl-1 expression within neural progenitors of the telencephalon and all neural progenitor cells, respectively (Arbour et al. 2008). Loss of Mcl-1 in neural progenitors resulted in widespread apoptosis throughout neural progenitor cells, migrating neuroblasts as well as newly born neurons within the cortical plate

(Arbour et al. 2008). Furthermore, studies in adult neural precursor cells show a two-fold increase in apoptotic cell death with the loss of expression of Mcl-1 (Malone et al. 2012). These findings provide evidence of the necessity for Mcl-1 within the specific regions of the CNS.

The requirement for Mcl-1 in the neural progenitor and newly born neuron populations has been well demonstrated within the developing telencephalon at time points of E12 and later. However, whether Mcl-1 is critical for survival at earlier time points or within other regions of the developing CNS has yet to be characterized.

1.9 Bcl-xL

Bcl-x can be alternatively spliced to form the shorter isoform Bcl-xS or the longer Bcl-xL. These two gene products have opposing actions where Bcl-xL acts as an anti-apoptotic protein and Bcl-xS is pro-apoptotic (Boise et al. 1993; Roth & D'Sa 2001). Within the developing CNS, the predominant gene product is Bcl-xL with very low levels of Bcl-xS being expressed (Krajewska et al. 2002). Bcl-xL expression begins in the CNS at approximately the onset of neurogenesis, E10.5 within the hindbrain and spinal cord, and is maintained at relatively high levels in the CNS throughout the remainder of the pre-natal period (Krajewska et al. 2002). By E13.5, expression of Bcl-xL is widespread through other populations of the CNS including the cortex, thalamus and hippocampus (Krajewska et al. 2002). Post-natally, Bcl-xL

also has elevatated expression throughout the CNS where it is thought to maintain survival of post-mitotic neurons (Krajewska et al., 2002; KA Roth et al., 2000; Savitt, Jang, Mu, Dawson, & Dawson, 2005).

Germline deletion of *bcl-x* is embryonically lethal at E13 with widespread death of immature post-mitotic neurons observed in the brainstem and rostral spinal cord (Motoyama et al. 1995). Roth and colleagues (1996) demonstrated *in vitro* that Bcl-x deficiency results in apoptosis of post-mitotic telencephalic neurons but does not affect the precursor cell population. Similar to *mcl-1*, early embryonic lethality of *bcl-x* germline deficient mice has led to the generation of several conditional KO models to study later developmental roles. Bcl-x has been shown to play a role in the survival of specific neuronal populations. A conditional KO model specific to catecholaminergic neurons resulted in the loss of one third of this cell population (Savitt et al. 2005). Additionally, KO models of Bcl-x specific to retinal ganglion cells and rod photoreceptors have demonstrated their requirement for Bcl-x within the visual system (Harder et al. 2012; Zheng et al. 2006). However, a complete CNS conditional knockout model of Bcl-xL that is specific to all neural-derived tissue of the CNS has yet to be created. Comprehensive study of the role of Bcl-xL in development of other neuronal populations therefore has yet to be examined.

1.10 Hypothesis and Aims

Of the main anti-apoptotic Bcl-2 family members it is known that A1, Bcl-w and Bcl-2 deficient animals have no apparent developmental defects in the CNS (Michaelidis et al. 1996; Hamasaki et al. 1998; Print et al. 1998; Ross et al. 1998). On the other hand, both Mcl-1 and Bcl-x have been examined to a limited extent in various model systems for their roles in neuronal survival (Arbour et al. 2008; Motoyama et al. 1995; Rinkenberger et al. 2000; Roth et al. 1996). The complete characterization of loss of *mcl-1* or *bcl-x* from all neural-derived tissue of the CNS has yet to be described. Given their redundency in binding partners amongst Bcl-2 pro-apoptotic proteins as well as their previously described roles in the survival of immature neurons, it is possible these two anti-apoptotic proteins may be capable of compensating at least partially for the loss of one another. *I hypothesize that Mcl-1 and Bcl-x have both distinct and overlapping roles in the regulation of cell survival during embryonic CNS development.* In this thesis, I have examined two main aims to address this hypothesis.

Aim #1:

To identify the roles of Mcl-1 and Bcl-x in the developing nervous system. Specifically, to determine when and where cell death is first observed and whether cell survival of specific neuronal populations is regulated by Mcl-1, Bcl-x or both.

Aim #2:

To identify potential Bcl-2 pro-apoptotic proteins functionally responsible for cell death observed in the *mcl-1* KO, *bcl-x* KO and double KO mice.

2.0 Materials and Methods

2.1 Mice

Mice were housed on a 12 hour light/dark cycle with access to food and water *ad libitum*. All experiments were approved by Memorial University's Animal Care Committee, adhering to the Guidelines of the Canadian Council on Animal Care.

Nestin Cre ($Cre^{+/-}$) mice were generated in the laboratory of Dr. R. Slack (Berube *et al.*, 2005), *mcl-1* floxed mice were generated in the laboratory of Dr. S. Korsmeyer (Opferman et al. 2005) and *bcl-x* floxed mice were generated in the laboratory of Dr. Hennighausen (Rucker et al. 2000). All strains were maintained on a C57BL/6 background.

Nestin Cre transgenic mice were bred with floxed mice to generate conditional knockout (KO) of *mcl-1* (MKO), *bcl-x* (BKO) as well as *mcl-1* and *bcl-x* double knockouts (DKO). Breeding pairs were placed in the same cage until the formation of a vaginal plug up to a maximum period of 3 days. In early morning and evening the female was checked for a vaginal plug, which at the point of discovery was designated embryonic day 0.5 (E0.5). Following formation of the plug, the weight of the female was monitored daily to verify pregnancy status.

Expected number of KO animals to determine Mendelian ratio was calculated by determining the probability of a KO embryo for each breeding pair multiplied by the total number of embryos collected from that litter. Probability of a KO embryo was determined based on the genotypes of the parents. An example calculation is shown in Appendix 1.

2.2 Genotyping

Embryonic mice were genotyped at the time of dissection from tissue samples collected from either the tail or limb buds. Adult mice were genotyped from tail clippings at the time of weaning. DNA was extracted using REDExtract-N-Amp tissue PCR kit (Sigma, XNAT2, Oakville, Ontario, Canada) and polymerase chain reaction (PCR) was completed on extracted DNA. PCR reaction components and conditions were followed as listed in tables 2.1 and 2.2. Following amplification, DNA samples were loaded and run in a 2% agarose gel (UltraPure Agarose – Invitrogen, 16500500, Burlington, Ontario, Canada) containing ethidium bromide (10mg/ml, Invitrogen, 15585-011, Burlington, Ontario, Canada) at 120V for approximately 30 minutes to detect the presence of the Cre allele and up to 90 minutes to separate *mcl-1* and *bcl-x* allele sizes. Gel bands were visualized under ultraviolet light and analyzed. *mcl-1* floxed alleles were indicated by a 400 base pair (bp) band and wild type alleles by a 360 bp band. Similarly, *bcl-x* floxed alleles displayed a 300 bp band, and wild type alleles a 200 bp band, while the presence of

Cre was indicated by a single band that was 700 bp. This allows for distinction of the possible genotypes as a wild type animal (*mcl-1*$^{+/+}$ or *bcl-x*$^{+/+}$) would only show the smaller band, floxed animals (*mcl-1*$^{f/f}$ or *bcl-x*$^{f/f}$) show only the larger band and heterozygotes (*mcl-1*$^{+/f}$ or *bcl-x*$^{+/f}$) show both bands.

Table 2.1: Reaction components for genotyping PCR.

Reagent	**Volume (µl/sample)**		
	Cre PCR	***mcl-1* PCR**	***bcl-x* PCR**
10X PCR Buffer	5	5	5
Primers (2.5 µM)	4	5	5
1.25 mM dNTPs	8	8	8
50mM $MgCl_2$	1.75	1.5	2
Taq Polymerase	0.5	0.5	0.5
Water	23.75	21	18.5
DNA sample	3	4	4
DMSO	N/A	N/A	2

Table 2.2: Reaction conditions for genotyping PCR.

Cre PCR		***mcl-1* PCR**		***bcl-x* PCR**	
94°C for 5 min		94°C for 5 min		94°C for 5 min	
94°C for 1 min 56°C for 1 min 72°C for 1.5 min	X30 cycles	94°C for 1 min 55°C for 1 min 72°C for 1 min	X30 cycles	94°C for 1 min 58°C for 1 min 72°C for 1.5 min	X30 cycles
72°C for 5 min		72°C for 1 min		72°C for 10 min	
10°C forever		10°C forever		10°C forever	

2.3 Tissue Collection and Preparation

At the time of sacrifice, pregnant dams were euthanized with an intraperitoneal injection of Euthanyl (250 mg/mL sodium pentobarbital-Vètoquinol, IEUS001, Lavaltrie, Quebec, Canada) followed by cervical dislocation.

The uterus was then removed and embryos were dissected and placed in individual dishes of cold 1X phosphate buffered saline (137 mM NaCl, 2.7 mM KCl, 10 mM Na_2HPO_4, 1.8 mM KH_2PO_4 (PBS)), pH 7.4. Embryos were then removed from their embryonic sacs and depending on the plane of sectioning (coronal or sagittal) the spinal column and brains were dissected out (coronal) or the embryo was left intact (sagittal) and fixed overnight in 4% paraformaldehyde (PFA) (pH 7.4) (Fisher Scientific, AC416785-000, Ottawa, Ontario, Canada). Following fixation, embryos were cryoprotected in a series of sucrose solutions (12%, 16%, 22% and 30% sucrose in 1X PBS). Brains and spinal cords were embedded in Tissue-Tek OCT Compound (Somagen Diagnostics, 4583, Sakura Finetek, California, United States) embedding medium and frozen in isopentane cooled on dry ice. Frozen tissue was stored at -80°C until the time of sectioning. Three to five embryos were collected and processed for each genotype and timepoint studied in this thesis.

All tissue was sectioned at 14 μm in thickness using a cryostat (Microm HM 520, Fisher Scientific, Ottawa, Ontario, Canada) at -23°C. Sections were collected on Superfrost Plus slides (Fisher, 1255015, Ottawa, Ontario, Canada) and stored at -80°C until further use.

2.4 Protein Extraction

E12 wild type Ctl, MKO and BKO forebrain, brainstem and spinal cord tissue for protein extraction was dissected in cold 1X PBS and immediately frozen on dry ice. Samples were then stored at -80°C until further use. Samples were lysed using complete immunoprecipitation (IP) buffer (25 mM Tris-Base pH 7.4, 148 mM NaCl, 1 mM $CaCl_2$, 1% Triton X-100, 0.2 mg/ml phenylmethylsulfonyl fluoride (PMSF), 10X protease inhibitors (aprotinin and leupeptin) and 10 mM dithiothreitol (DTT)). Protein concentration of the lysate was measured in duplicate using Bio-Rad Protein Determination Assay reagent (Bio-Rad, 500-0006, Mississauga, Ontario, Canada) based on the Bradford assay (Table 2.3). Using the slope of the curve generated from the absorbance values of known standards, the protein concentration was determined for each sample.

Table 2.3: Bradford assay standard curve.

Sample	ddH_2O (µL)	0.5 µg/µL BSA Standard (µL)	Bio-Rad Reagent (µL)	Approximate Absorbance
Standard 1	800	0	200	0.000
Standard 2	795	5	200	0.150
Standard 3	790	10	200	0.300
Standard 4	785	15	200	0.450
Sample (5 µL)	795	-	200	

2.5 Western Blotting

Samples were prepared by adding a volume containing 30 µg of protein to 5 µl of 5X protein loading buffer and topped up to a total volume of 25 µl with IP buffer. Samples were then boiled for 2 minutes to denature and loaded into a 15% poly-acrylamide gel (Table 2.4). One well of each gel was loaded with 10 µl of Precision Plus Protein Kaleidoscope standard (Bio-Rad, 161-0375, Mississauga, Ontario) as a reference for protein sizes.

Table 2.4 Poly-acrylamide separating and stacking gel recipes.

15% Separating Gel	
ddH_2O	4.5 ml
0.5 M Tris, 1.5 M glycine	4.0 ml
10% SDS	0.8 ml
50% glycerol	2.0 ml
40% acrylamide; 0.25% bisacrylamide	7.0 ml
Ammonium persulphate	30 mg in 1 ml ddH_2O
10% TEMED	0.02 ml
4% Stacking Gel	
ddH_2O	4.05 ml
0.5 M Tris-HCl pH 6.8	1.4 ml
10% SDS	0.4 ml
50% glycerol	1.0 ml
40% acrylamide, 0.25% bisacrylamide	1.25 ml
Ammonium persulphate	25 mg in 1 ml ddH_2O
10% TEMED	0.01 ml

The gel was run using a Mini-PROTEAN apparatus (Bio-Rad, 165-8001, Mississauga, Ontario, Canada) containing running buffer (0.1 M Tris-Base, 0.3 M glycine, 0.01 M SDS). Samples were run at 80 V until they had cleared the stacking gel and then at 110V until the dye had run to the bottom of the separating gel. Proteins were then transferred to a nitrocellulose membrane (Amersham

BioSciences, RPN30320, Piscataway, New Jersey, USA) using a Bio-Rad Mini Trans-Blot Electrophoretic Transfer Cell (Bio-Rad, 170-3930, Mississauga, Ontario, Canada) containing transfer buffer (0.02 M Tris-Base, 0.15 M glycine and 4.9 M methanol). The protein transfer was run at 290 A for 1 to 1.5 hours. The membrane was then washed in 1X Tween-20 phosphate buffered saline (TPBS) (126 mM NaH_2PO_4, 620 mM NaCl, 4 mM Tween-20) at room temperature for 2X 10 minutes, followed by 1 hour of blocking in 5% blotto (5% skim milk powder in 1X TPBS). Next, the membrane was washed in 0.5% blotto for 5 minutes and then incubated in primary antibody (Table 2.5) diluted in 0.5% blotto overnight at 4°C. The following morning the membrane was washed in 1X TPBS for 10 minutes, then 0.5% blotto for 5 minutes, followed by 1 hour incubation in the appropriate secondary antibody at a concentration of 1:2000 diluted in 0.5% blotto. Next, the membrane was washed 3 times for 10 minutes with 1X TPBS and the secondary antibody was detected using a chemiluminescence reaction kit (Perkin Elmer Labs Inc., 02118-2512, Waltham, Massachusetts, USA) according to the manufacturer's instructions. Images were captured using a GE ImageQuant LAS 4000 (GE Healthcare, 28-9558-10, Baie d'Urfe, Quebec, Canada). Additional proteins were examined on the same membrane by stripping the membrane using Western Blot Stripping Buffer (Sigma, 21059, Oakville, Ontario, Canada). Blots were incubated in the stripping buffer for 30 minutes at 37°C. Blots were washed 3 times in 1X TPBS for 5 minutes each then the procedure was continued as previously described beginning with blocking the membrane. β-actin expression was used as a loading control for all blots.

Table 2.5: List of antibodies used for western blot analysis.

Protein	Concentration	Source
β-Actin	1/5000	A5316, Sigma, Oakville, Ontario, Canada
Bcl-x	1/1000	Cell Signaling Technology, 2764, Beverly, Massachusetts, United States
Mcl-1	1/1000	600-401-394, Rockland, Limerick, Pennsylvania, United States

2.6 Cresyl Violet Staining

Every 10th tissue section (140 μm apart) was collected and stained using cresyl violet. Slides were warmed at 37°C for 20 minutes prior to treatment. Embryonic sections were placed in 0.1% cresyl violet stain (Sigma, C1791-5G, Oakville, Ontario, Canada) for 20 minutes, following which they were washed in fresh tap water for 1 minute. The slides were dehydrated through a series of ethanols (50%, 70%, 90%, 95%, 100% X3) for 30 seconds each, followed by 30 seconds in isopropanol and finally 2X 30 seconds in toluene. Slides were mounted using Permount (Fisher, SP15-500, Ottawa, Ontario, Canada) and coverslipped.

2.7 Immunohistochemistry

Slides were warmed at 37°C for 20 minutes and a hydrophobic barrier (Dako pen- Dako Canada, S2002, Burlington, Ontario, Canada) was drawn around tissue sections prior to treatment. Slides were then washed in 1X PBS and then incubated overnight in primary antibody solution (Table 2.6) diluted in 1X PBS at room temperature in a humid chamber. The following morning slides were washed in 1X PBS and incubated with the secondary antibody for 1 hour at room temperature. Finally slides were stained with the nuclear dye, Hoechst (1:250 BisBenzimide H33258- Sigma, B1155, Oakville, Ontario, Canada) diluted in 1X PBS for 2 minutes and washed in 1X PBS again. Slides were then coverslipped using 1:3 glycerol:1X PBS solution, sealed with nail polish and stored at -20°C.

Slides pre-treated using antigen retrieval technique were brought to a boil in 10 mM sodium citrate and then immediately cooled in the sodium citrate by placing the copelin jar in ice water for 5 minutes. This procedure was repeated 2 more times, after which slides were washed in 1 X PBS and the appropriate primary antibody was applied.

Table 2.6: List of antibodies for immunohistochemistry.

Primary Antibody	Tissue Pre-treatment	Concentration (antibody:1X PBS)	Source
Active Caspase 3	n/a	1/400	BD Biosciences, 559565, Mississauga, Ontario, Canada
BrdU	3 min acetone 30 min 37°C 2N HCl	1/100	BD Biosciences, 347580, Mississauga, Ontario, Canada
Bcl-x	Antigen Retrieval	1/200	Cell Signaling Technology, 2764, Beverly, Massachusetts, United States

2.8 Microscopy

All immunostained slides were viewed using a Zeiss AxioImager Z.1 microscope (Carl Zeiss Microscopy, Jenna, Germany) and fluorescence produced using a Colibri LED light source (Carl Zeiss Microscopy, Jenna, Germany). Photomicrographs were taken using a Zeiss AxioCam MRm camera (Carl Zeiss Microscopy, Jenna, Germany) using Zeiss AxioVision v4.8 software. Low magnification images were taken using a Zeiss Stemi-2000 dissecting microscope (Carl Zeiss Microscopy, Jenna, Germany) and Zeiss AxioCam MRm camera (Carl Zeiss Microscopy, Jenna, Germany).

2.9 Quantitative Reverse Transcription PCR

RNA was extracted separately from dissected forebrain, brainstem and spinal cord tissue from E10 and E12 wild type CD1 mice. E10 samples were pooled from

3 embryos, while E12 samples were from individual embryos. Total RNA was extracted using TRIzol Reagent (Life Technologies, 15596-026, Burlington, Ontario, Canada) according to the manufacturer's instructions. All RNA samples were then DNase treated by adding 1 μl 10X DNase 1 reaction buffer (Invitrogen, y02340, Burlington, Ontario, Canada), 1 μl DNase 1 amplification grade enzyme (Invitrogen, 18068-015, Burlington, Ontario, Canada) to 1 μg of RNA and topping up to a total volume of 9 μl using diethyl pyrocarbonate (DEPC) H_2O. Following a 15 minute incubation at room temperature, the reaction was stopped with the addition of 1 μl of 25 mM ethylenediaminetetraacetic acid (EDTA) and incubated at 65°C for 1 minute. RNA concentration and purity was measured using a Thermo Scientific NanoDrop 1000 spectrophotometer (Waltham, Massachusetts, USA). All samples were stored at -80°C until further use.

Complementary DNA (cDNA) synthesis was completed using the RevertAid H Minus first strand cDNA Synthesis kit (Thermo Scientific, K1631, Waltham, Massachusetts, USA) according to the manufacturer's instructions. 400 ng of total RNA was used for cDNA synthesis, and cDNA concentration was measured following synthesis to ensure equivalent amplification across samples.

Quantitative real time PCR (qRT-PCR) was performed using StepOnePlus Real-Time PCR System (Life Technologies, Burlington, Ontario, Canada). Prior to gene quantification, all qPCR primers were validated using a standard curve with

control E13 whole brain cDNA samples. All primer sets met an efficiency score between 90-110%. To quantify the level of expression of individual *bcl-2* family genes, equal amounts of cDNA were synthesized from total extracted RNA. cDNA was mixed with Power SYBR Green PCR master mix (Life Technologies, 4367659, Burlington, Ontario, Canada) according to manufacturer's instructions with 0.4 µl of 10 µM forward and reverse primers (Table 2.7). Quantification of genes for each sample was done in triplicate. Glyceraldehyde 3-phosphate dehydrogenase (GAPDH) was amplified as an internal positive control, negative control wells with the absence of cDNA template as well as RNA only wells were used to verify lack of genomic contamination.

Table 2.7: List of qRT-PCR forward and reverse primers.

Name	Accession #	Forward (5'-3')	Reverse (5'-3')	Reference
gapdh	NM_008084	Unknown sequence	Unknown sequence	Qiagen, QT01658692
mcl-1	NM_008562.3	Unknown sequence	Unknown sequence	Qiagen, QT00107436
bcl-x	NM_009743.4	Unknown sequence	Unknown sequence	Qiagen, QT00149254
bcl-w	NM_007537	ACCCAGGTTTCCGACGAAC	TTGTTGACACTCTCAGCACAC	PrimerBank 6680773c2
noxa	NM_021451.2	CACCGGACATAACTGTGGTT	TTGAGCACACTCGTCCTTCA	Wilson et al., 2013
bak	NM_007523.2	CAACCCCGAGATGGACAACTT	CGTAGCGCCGGTTAATATCAT	PrimerBank 15553445a1
bim	NM_207680.2	CGACAGTCTCAGGAGGAACC	CATTTGCAAACACCCTCCTT	Zamorano et al., 2012
bad	NM_007522.2	AAGTCCGATCCCGGAATCC	GCTCACTCGGCTCAAACTCT	PrimerBank 6671610a1
puma	NM_133234.2	ACGACCTCAACGCGCAGTACGA	GGAGGAGTCCCATGAAGAGATTGT	Gao et al., 2010

bax	NM_007527.3	TGAAGACAGGGGCCTTTTTG	AATTCGCCGGAGACACTCG	PrimerBank 6680770a1
bid	NM_007544.3	CCAGTCACGCACCATCTTTG	GTCCATCTCGTTTCTAACCAAGT	PrimerBank 77404282c3

Gene expression levels were quantified relative to expression levels in wild type E13 whole brain tissue using the comparative CT (threshold cycle) method. This consisted of first calculating the mean CT of the triplicates, then calculating the ΔCT relative to the selected housekeeping gene GAPDH. From there the ΔΔCT was determined and finally the relative quantity (RQ) ($RQ=1/2^{(\Delta\Delta CT)}$) was calculated and evaluated (Appendix 2).

2.10 *In situ* Hybridization

Lyophilized riboprobe plasmids were received from various laboratories as indicated in Table 2.9 or newly designed and synthesized. Synthesized probes were designed following the protocol used by the Allen mouse atlas (Allen Mouse Brain Atlas, 2011). RNA was extracted from whole brains from E13-E15 C57Bl/6 embryos and cDNA was synthesized following the same protocol described for qPCR experiments. Primers were designed according the Allen mouse atlas protocol (Allen Mouse Brain Atlas, 2011) and synthesized by Integrated DNA Technologies (Coralville, Iowa, United States). PCR reaction components and conditions were followed as listed in Table 2.8. PCR products were run in a 4% agarose gel and the targeted DNA fragments were cut out and purified using Illustra GFX PCR DNA and gel band purification kit (GE Healthcare Life Sciences, 28-9034-70, Mississauga, Ontario, Canada) according to the manufacturer's instructions. DNA was resuspended in 25 µl 10 mM Tris HCl (pH 8.0) and its

concentration was determined using a Qubit fluorometer (Q32857, Invitrogen, Burlington, Ontario, Canada). Ligation of the PCR product was completed using pGEM-T Easy vector system (Fisher Scientific, Pr-A1360, Ottawa, Ontario, Canada) according to the manufacturer's instructions. The remainder of the procedure was completed in the same way for both synthesized and riboprobes received from other laboratories.

Table 2.8: PCR reaction components and conditions for Noxa riboprobe synthesis.

Reagent	Volume (µl)	Reaction Conditions	
10X PCR Buffer	5	94°C for 5 min	
Primers (2.5µM)	5	94°C for 1 min	X30 cycles
1.25mM dNTPs	8	58°C for 1 min	
50mM $MgCl_2$	1.5	72°C for 1.5 min	
Taq Polymerase	0.5	72°C for 10 min	
Water	24	10°C forever	
cDNA	1		

Plasmids were resuspended in Tris-EDTA (TE) buffer and transformed into Subcloning Efficiency DH5α competent cells (Invitrogen, 18265-017, Burlington, Ontario, Canada). Bacteria were grown on ampicillin- (Invitrogen, 11593027, Burlington, Ontario, Canada) containing agar plates (LB Agar EZMix- Sigma, L7533, Oakville, Ontario, Canada) and incubated at 37°C overnight. Isolated colonies were picked and grown in 3 ml of LB broth (Sigma, L7658, Oakville, Ontario, Canada) containing ampicillin (Invitrogen, 11593027, Burlington, Ontario, Canada) overnight at 37°C. A Miniprep kit (Qiagen, 27104, Toronto, Ontario, Canada) was used to isolate plasmids according to the manufacturer's instructions. Plasmids

were digested with restriction enzymes overnight at 37°C. Enzyme sites were selected within and outside the riboprobe insert to verify the riboprobe insert. The following day digested plasmids were run in a 0.8% agarose (UltraPure Agarose – Invitrogen, 16500500, Burlington, Ontario, Canada) gel to ensure expected band sizes were present and there was no contamination. All riboprobes were also sent for sequencing at the Centre for Applied Genomics at Sick Kids hospital (Toronto, Ontario, Canada). After confirmation of the proper plasmid construct, larger 400 ml LB broth (Sigma, L7658, Oakville, Ontario, Canada) cultures were incubated overnight at 37°C and Maxiprep (Qiagen, 12963, Toronto, Ontario, Canada) plasmid isolation was performed according to the manufacturer's instructions.

Table 2.9: Sources of *bcl-2* family riboprobes.

Gene	Source
bim	Dr. S. Korsmeyer Lab
bmf	Dr. R. Slack Lab
bax	Dr. M. O'Reilly Lab
noxa	Synthesized

Isolated plasmids were purified using Illustra GFX DNA Purification Kit (GE Life Sciences, 28-9034-70) according to the manufacturer's instructions. DNA concentration was determined using a Qubit fluorometer (Invitrogen, Q32857, Burlington, Ontario, Canada). 1 μg of plasmid was linearized overnight using restriction enzyme digest and DIG labeling was completed the following day using DIG RNA Labeling Mix kit (Roche, 11277073910, Mississauga, Ontario, Canada) according to the manufacturer's instructions. Labeling efficiency was tested by

performing a spot assay with 10 fold serial dilutions of the DIG-labeled riboprobe spotted onto Hybond nylon membrane (Amersham BioSciences, RPN30320, Piscataway, New Jersey, USA), dried and UV cross linked. The membrane was then washed in DIG detection buffer 1 (100 mM Tris pH 7.5, 150 mM NaCl) for 5 minutes, then blocked with 1% blocking reagent (Roche, 11096176001, Mississauga, Ontario, Canada) in DIG detection buffer 1 for 30 minutes. Following blocking, a 1:2000 dilution of anti-DIG antibody (Roche, 11093274910, Mississauga, Ontario, Canada) was added to the blocking solution and washed for 30 minutes at room temperature with rocking. The membrane was then washed with DIG detection buffer 1 twice for 15 minutes each and DIG detection buffer 2 (100 mM Tris pH 9.5, 100 mM NaCl, 50 mM MgCl2) twice for 5 minutes each. Finally the membrane was incubated in colour development solution (0.45% 4-Nitroblue tetrazolium (NBT), 0.35% 5-bromo-4-chloro-3-indolyl-phosphate (BCIP) in DIG detection buffer 2) in the dark at room temperature for 30 minutes. The reaction was stopped by washing the membrane in tap water and allowing it to dry. Labeled probes were then assessed by comparing the signal intensities of the dots.

Tissue sections were warmed to room temperature for 30 minutes, and then incubated in 1:50 to a 1:5000 dilution of denatured riboprobe in hybridization solution (Table 2.9). The dilution of riboprobe was determined by the signal intensities from the spot assay to ensure equal dilutions of sense and antisense probes were added to tissue samples. Any sense and antisense probes that had

greater than a 10 fold difference in labeling intensity were discarded and fresh probes were relabeled. Sections were incubated with riboprobes at 65°C in a humidity chamber overnight. The following morning slides were incubated in wash buffer (Table 2.10) at 65°C with rocking for 1X 15 minutes and 2X 30 minutes. Slides were then transferred to 1X MABT (0.5 M Maleic acid, 0.75 M NaCl, 0.5% Tween 20) and washed at room temperature for 30 minutes. A hydrophobic barrier was drawn around sections on the slides with a Dako pen (Dako Canada, S2002, Ontario, Canada) and sections were incubated in blocking solution (20% heat-inactivated horse serum, 2% blocking reagent in 1X MABT) in a humidified chamber for 1 hour at room temperature. Blocking solution was removed and 200 μl of anti-DIG antibody (Roche, 11093274910, Mississauga, Ontario, Canada) diluted 1:1000 in blocking solution was added to the slides and incubated in the humidity chamber at room temperature overnight. The next morning slides were washed 5X 20 minutes in 1X MABT at room temperature. Sections were equilibrated in pre-staining buffer (Table 2.11) 2X 10 minutes at room temperature. Slides were then incubated in 30 ml of staining buffer with NBT (4.5 μl/ml staining buffer) (Roche, 1383213, Mississauga, Ontario, Canada) and BCIP (3.5 μl/ml staining buffer) (Roche, 11383221001, Mississauga, Ontario, Canada) in the dark at room temperature for 3-24 hours. All sense and antisense probes of the same gene were incubated for the same amount of time. The reaction was stopped by washing slides in PBS, 2X 5 minutes. Sections were covered in 1:1 glycerol/PBS and coverslipped using nail polish to seal the edges. Slides were stored at -20°C until further use.

Table 2.10: Hybridization solution recipe.

Reagent	Volume (10 ml)
1X Salt	1 ml of 10X
Deionized Formamide	5 ml
10% Dextran Sulfate	2 ml of 50%
rRNA (1mg/ml)	1 ml of 10mg/ml
1X Denhardt's	100 μl of 100X
H_2O	900 μl

Table 2.11: *In situ* hybridization wash buffer recipe.

Reagent	Volume (500 ml)
1X SSC	25 ml of 20X
Deionized Formamide	250 ml
0.1% Tween-20	500 μl
H_2O	224.5 ml

Table 2.12: *In situ* hybridization staining buffer recipe.

Reagent	Volume (301.3 ml)
100 mM NaCl	6 ml of 5M
50 mM $MgCl_2$	15 ml of 1M
100 mM Tris pH 9.5	30 ml of 1M
0.1% Tween-20	300 μl
dH_2O	250 ml

3.0 Results

3.1 Nestin Cre selectively deletes *mcl-1* and *bcl-x* from the CNS.

To identify the roles of Mcl-1 and Bcl-x throughout the developing CNS, mice expressing Cre recombinase under control of the Nestin promoter were used to excise floxed *mcl-1* and *bcl-x* genes. Nestin is expressed in neural precursor cells by E7.5 (Lendahl, 1990), well before the onset of neurogenesis at E10 (Angevine & Sidman, 1961; Nornes & Carry, 1978). Only neural precursor cells and their progeny have the floxed genes excised, resulting in a CNS-specific conditional knockout model. To examine the expression of Mcl-1 and Bcl-x proteins, immunohistochemistry and western blotting were performed (Figure 3.1). Immunohistochemistry for Bcl-x was performed on sagittal sections through the brain and spinal cord of E13 Ctl and BKO embryos. In Ctl embryos, Bcl-x had limited expression throughout regions of proliferative populations but was present throughout the rest of the CNS (Figure 3.1A) consistent with previous studies (Motoyama et al. 1995). In contrast, there was a marked decrease of Bcl-x expression throughout the BKO CNS (Figure 3.1A). Western blotting analysis of cell lysate from E12 Ctl, Het and BKO forebrain, brainstem and spinal cord tissue, confirmed significantly reduced expression of Bcl-x in all regions of the CNS of both Het and BKO mice (Figure 3.1B). Loss of Mcl-1 expression in this MKO model has been previously demonstrated (Arbour et al., 2008). Here E12 MKO forebrain,

brainstem and spinal cord cell lysate confirmed greatly reduced or absent expression of Mcl-1. Taken together these results demonstrate efficient deletion of *mcl-1* and *bcl-x* throughout the neural-derived CNS tissue of KO embryos.

Figure 3.1: BKO and MKO animals have diminished expression of Bcl-x and Mcl-1.

(A) Representative photomicrographs of Bcl-x immunohistochemistry on sagittal sections through the brain (top panels) and spinal cord (bottom panels) of E13 Ctl and BKO embryos. Reduced Bcl-x expression is seen throughout the CNS of BKO embryos. **(B)** Western blot analysis of Bcl-xl protein expression from E12 Ctl, Het and BKO forebrain (Fb), brainstem (Bs) and spinal cord (Sp) tissue (n=3). **(C)** Western blot analysis of Mcl-1 protein expression from E12 Ctl, Het and MKO Fb, Bs and Sp tissue (n=2). Quantification of **(D)** Bcl-xL and **(E)** Mcl-1 expression from western blot analysis. Error bars indicate standard error of the mean (SEM). ***$p < 0.001$, *$p < 0.05$.

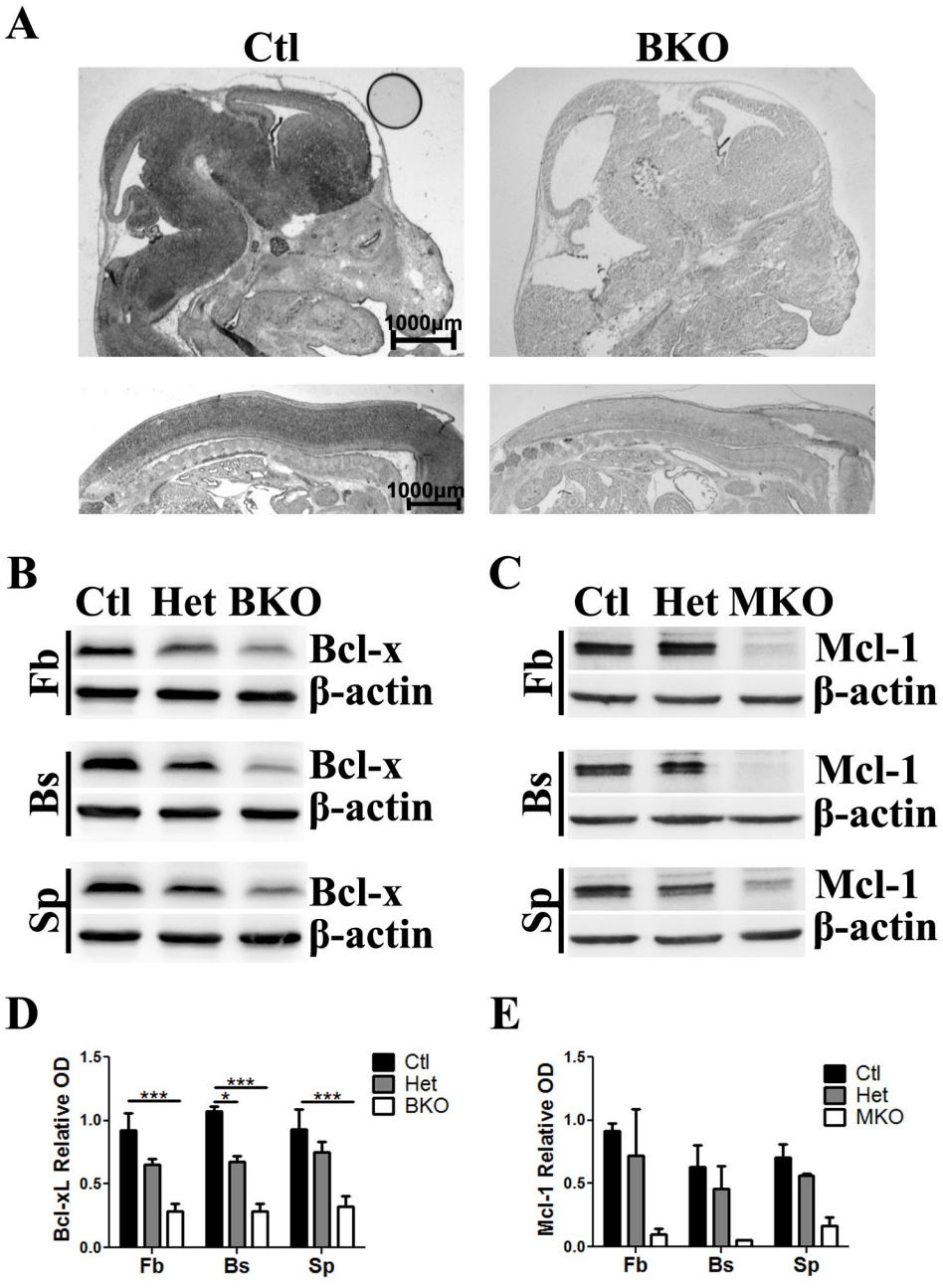
A
Ctl
BKO
1000μm
1000μm
B
Ctl Het BKO
Fb
Bcl-x
β-actin
Bs
Bcl-x
β-actin
Sp
Bcl-x
β-actin
C
Ctl Het MKO
Fb
Mcl-1
β-actin
Bs
Mcl-1
β-actin
Sp
Mcl-1
β-actin
D
Bcl-xL Relative OD
1.5
1.0
0.5
0.0
***
***
*
***
Ctl
Het
BKO
Fb
Bs
Sp
E
Mcl-1 Relative OD
1.5
1.0
0.5
0.0
Ctl
Het
MKO
Fb
Bs
Sp

3.2 Mcl-1 and Bcl-x are required for spinal cord development.

To examine the impact of the deletion of *mcl-1* and *bcl-x*, histology was performed on spinal cord, brainstem and forebrain tissue sections from MKO and BKO embryos. Specifically, cresyl violet and hoechst staining as well as immunohistochemistry labeling active caspase-3-expressing cells were used on tissue sections from embryonic time points E10, E11, E12, E13 and E15. Three to five embryos of each genotype were analyzed for each time point studied.

To examine the loss of Mcl-1 and Bcl-x on early spinal cord development, tissue histology was performed examining the spinal cord region shown in Figure 3.2A. Apoptotic cell death began in the spinal cord in both MKO and BKO embryos at E10 whereas very little or no cell death was observed in Ctl animals (Figure 3.2B). Apoptosis In the MKO, apoptosis was extensive along the ventral spinal cord at E10. A dramatic switch occurred by E11, where cell death was observed more concentrated along the length of the dorsal spinal cord. In contrast, minimal apoptosis was observed in the BKO spinal cord at E10. By E11 (Figure 3.2B) through E13 (Figure 3.2D) apoptosis began to spread dorsally, but remained predominantly along the ventral spinal cord. E13 cresyl violet coronal tissue sections revealed a reduced size of the MKO spinal cord (Figure 3.2C). Although not quantified, this reduction in diameter in the MKO was consistently observed throughout MKO

animals, while no obvious size difference was seen in the BKO spinal cord at this time. Coronal tissue sections also revealed the difference in pattern of cell death that was seen at E13 (Figure 3.2D). At this time point, apoptosis was limited to the dorsal spinal cord in the MKO and primarily the ventral spinal cord in the BKO. Apoptosis was greatly reduced in the BKO by E15 and there was no longer an apparent increased level of cell death along the ventral aspect of the spinal cord (Figure 3.2E). Apoptotic cell death occurred in the spinal cord of both MKO and BKO embryos by E10, but progressed in a different pattern suggesting distinct populations were affected.

Figure 3.2: Onset of cell death in the developing spinal cord of MKO and BKO mice.

(A) Cresyl violet-stained sagittal sections of whole E10 and E13 wild type embryos highlighting region examined in black box. **(B)** Representative photomicrographs of active caspase-3 (AC3) immunohistochemistry staining showing apoptotic cell death in sagittal sections of the spinal cord of E10 and E11 Ctl, MKO and BKO embryos. D=dorsal, V=ventral, R=rostral, C=caudal. **(C, D)** Representative photomicrographs of E13 coronal spinal cords from Ctl, MKO and BKO embryos. Cresyl violet (CV) staining shows tissue histology **(C)**, while active caspase-3 immunohistochemistry labels apoptotic cells **(D)**. **(E)** Photomicrographs of coronal spinal cords from E15 Ctl and BKO embryos stained for active caspase-3 indicate reduced apoptotic cell death in BKO animals by this time point.

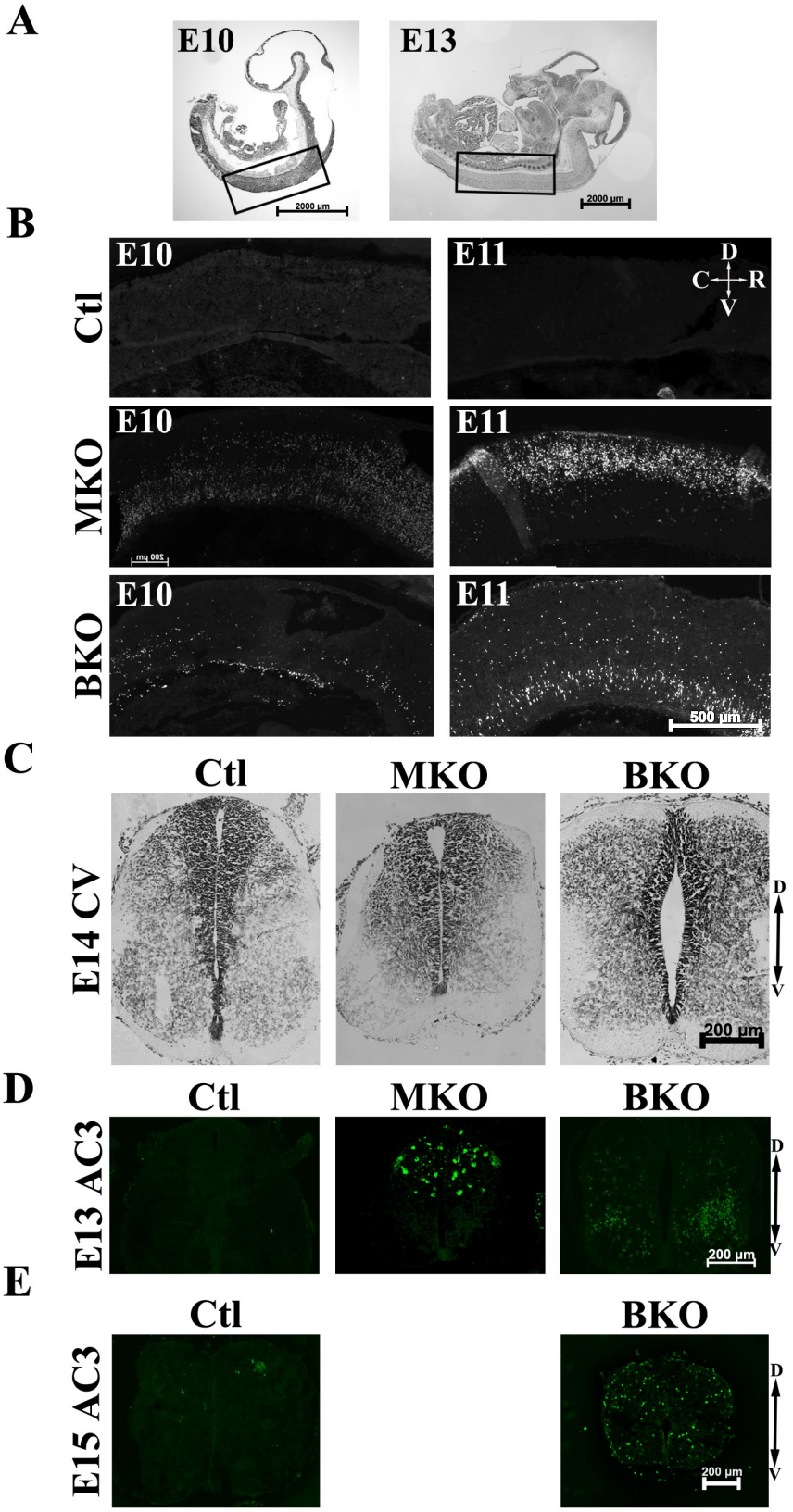
A
E10
E13
2000 µm
2000 µm
B
Ctl
MKO
BKO
E10
E11
D
C
R
V
500 µm
C
Ctl
MKO
BKO
E14 CV
D
V
200 µm
D
Ctl
MKO
BKO
E13 AC3
D
V
200 µm
E
Ctl
BKO
E15 AC3
D
V
200 µm

3.3 Mcl-1 and Bcl-x are required for brainstem development.

Given the early onset of cell death in the spinal cord, next the progression of apoptosis was examined in the brainstem, another early developing region of the CNS. To characterize the pattern of cell death of the MKO and BKO brainstem, histology was performed on E10- E13 tissue (Figure 3.3). Sagittal sections through the brainstem revealed similar timing in the onset of cell death to that in the spinal cord (Figure 3.3C). In both the MKO and BKO, apoptosis was observed in the brainstem at E10 and progressed through E11 (Figure 3.3C). By E11 the ventricular zone population underwent apoptosis in the MKO, but in the BKO these cells were spared and apoptotic cells were located in the apical region (Figure 3.3C).

Cresyl violet-stained cross sections at the level of the facial motor nucleus (FMN) demonstrated condensed cell bodies indicative of apoptosis in the BKO FMN. The FMN in both MKO and BKO animals appeared to be reduced in size (Figure 3.3D). This suggested a role for Mcl-1 and Bcl-x in the survival of motor neurons or their precursors in the brainstem. Sagittal sections of the BKO brainstem revealed the level of apoptosis progressed until E13, which coincides with apoptosis seen in the spinal cord (Figure 3.3E). Both Mcl-1 and Bcl-x are required for the survival and development of the brainstem by E10.

Figure 3.3: Onset of apoptotic cell death in the MKO and BKO brainstem.
(A) Cresyl violet-stained sagittal sections of whole E10 and E13 wild type embryos highlighting region examined in black box. **(B)** High magification photomicrograph of cresyl violet stained E13 Ctl brainstem showing orientation of apical (A) and basal (B) surfaces. **(C)** Representative photomicrographs of active caspase-3 immunohistochemistry showing apoptotic cell death in sagittal sections of the brainstem of E10 and E11 Ctl, MKO and BKO embryos. Arrows indicate ventricular zone. **(D)** Representative photomicrographs of E13 coronal brainstems from Ctl, MKO and BKO embryos at the level of the facial motor nuclei. Cresyl violet (CV) staining shows tissue histology. Dashed lines outline the FMN and arrows indicate apoptotic cell bodies. **(E)** Photomicrographs of sagittal brainstem sections from E13 Ctl and BKO embryos stained for active caspase-3 indicate continued apoptotic cell death in BKO animals at E13. A= apical, B= basal, R= rostral, C= caudal, V= ventral, D= dorsal.

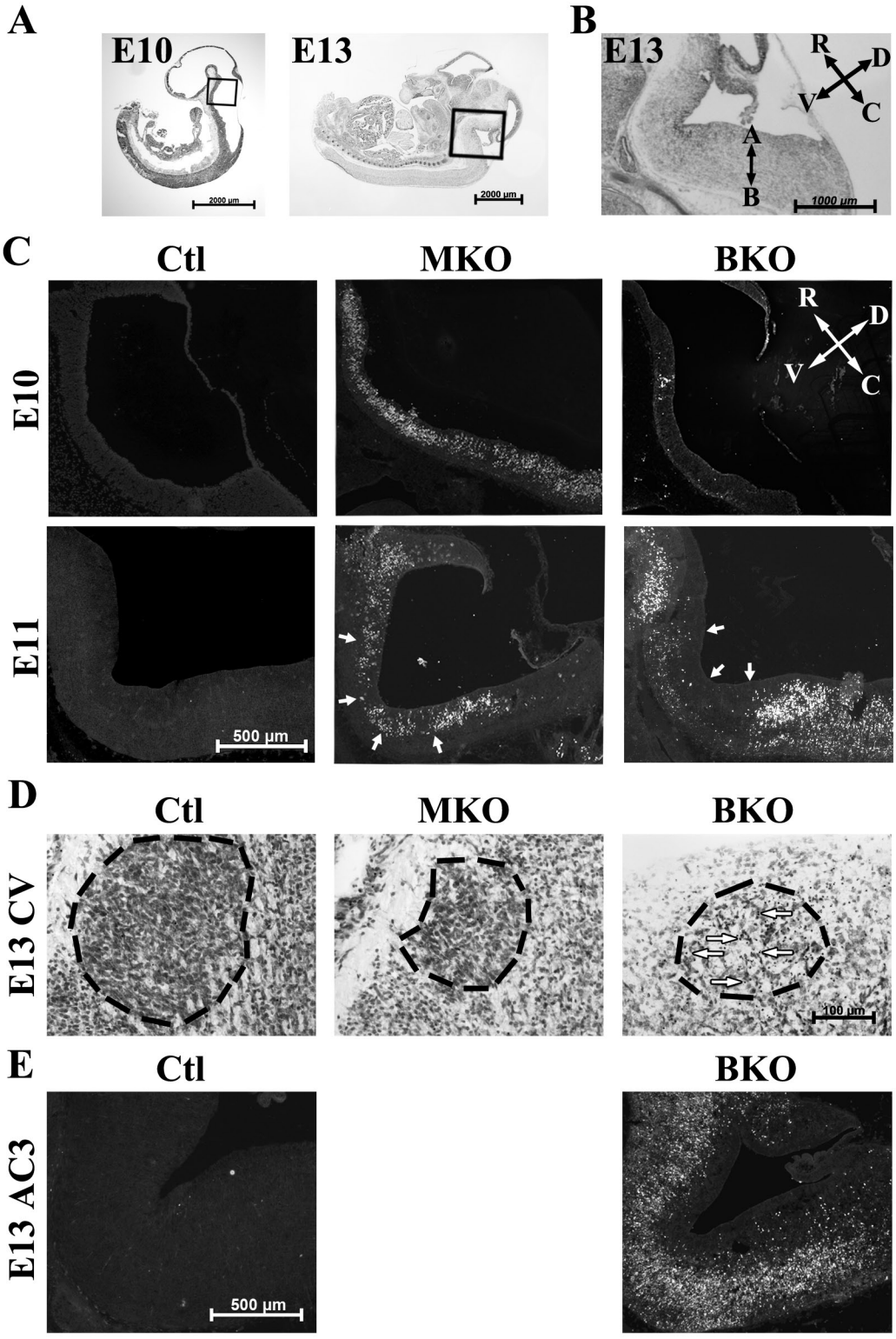
A
E10
E13
2000 µm
2000 µm
B
E13
R
D
V
C
A
B
1000 µm
C
Ctl
MKO
BKO
E10
R
D
V
C
E11
500 µm
D
Ctl
MKO
BKO
E13 CV
100 µm
E
Ctl
BKO
E13 AC3
500 µm

3.4 Mcl-1 is required for early forebrain development

Next, to evaluate the impact of the loss of Mcl-1 on the development of the forebrain, tissue histology was performed. Apoptotic cell bodies were present throughout sagittal and coronal sections of the E10, E11 and E12 MKO forebrain (Figure 3.4). Similar to other regions of the CNS, apoptosis was first seen within the subpallium, developing thalamus and prethalamus of the MKO forebrains at E10 (Figure 3.4A). Apoptosis was seen earlier than has been previously reported in the developing forebrain (Arbour et al. 2008). By E11, cell death had spread throughout the entire forebrain (Figure 3.4A). Cresyl violet-stained sections from E12 embryos revealed condensed cell bodies throughout all layers of the developing cortex (Figure 3.4B). E12 active caspase-3 immunohistochemistry on coronal tissue sections revealed cell death throughout the width of the E12 cortex (Figure 3.4C). These results are consistent with previous findings where *mcl-1* deletion resulted in apoptosis of cells at each stage of neurogenesis from neural precursor cell to immature neuron (Arbour et al., 2008). The early developing forebrain requires Mcl-1 for cell survival and development.

Figure 3.4: Onset of apoptotic cell death in the MKO forebrain.

(A) Representative photomicrographs of apoptotic cell death in E10 and E11 Ctl and MKO sagittal forebrains as labeled by active caspase-3 immunohistochemistry. Apoptosis is seen in the MKO forebrain as early as E10. **(B,C)** Representative photomicrographs of coronal E12 cortices from Ctl and MKO embryos. Cresyl violet-staining reveals tissue histology **(B)** and active caspase-3 immunohistochemistry labels apoptotic cells **(C)**. Arrows indicate apoptotic cells with condensed cell bodies in cresyl violet stained sections. Thal= developing thalamus, PThal= prethalamus, SPal= subpallium, L= lateral, M= medial, V= ventral, D= dorsal, P= posterior, A= anterior.

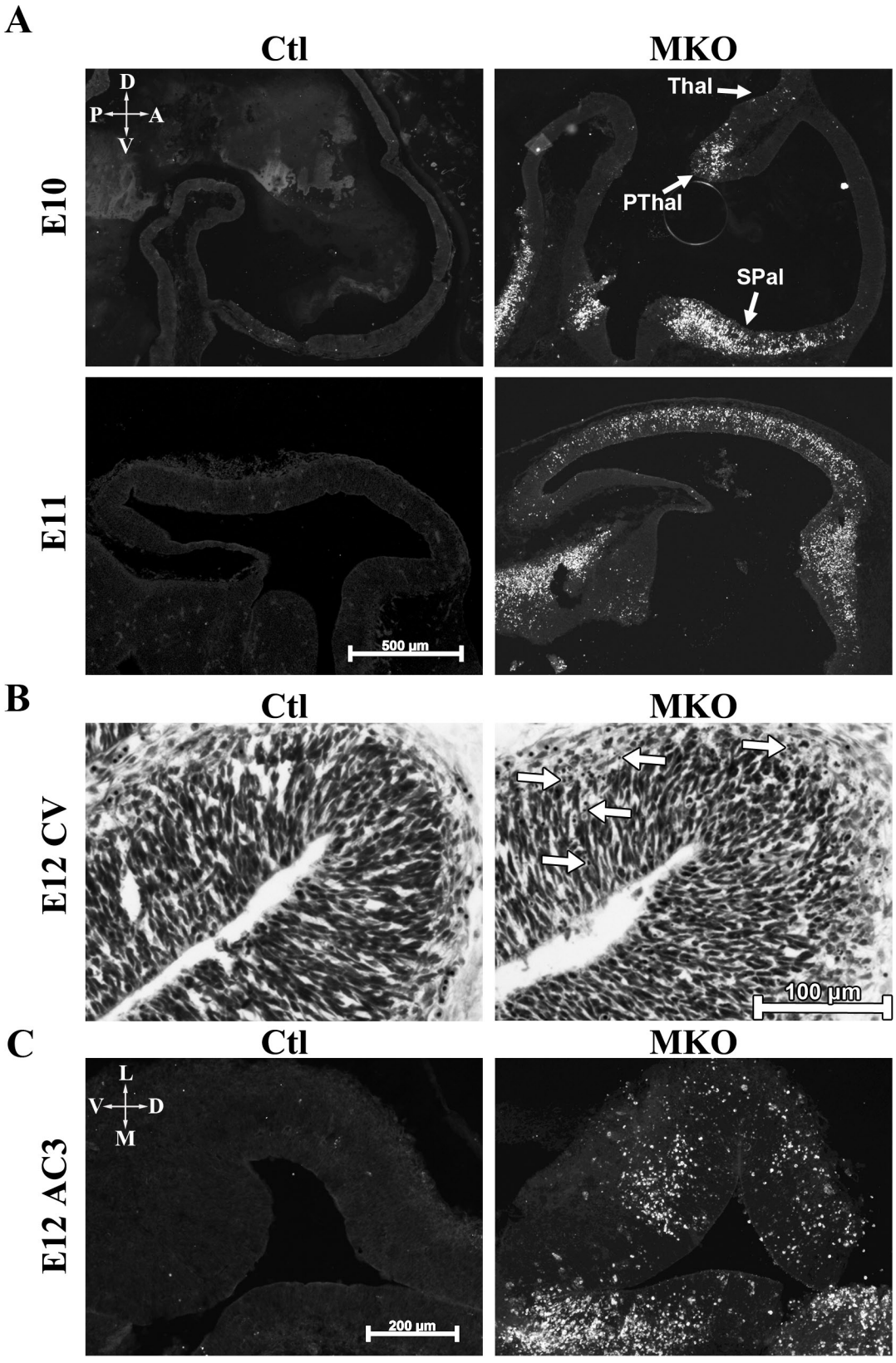
A
Ctl
MKO
D
P
A
V
Thal
PThal
SPal
E10
E11
500 µm
B
Ctl
MKO
E12 CV
100 µm
C
Ctl
MKO
L
V
D
M
E12 AC3
200 µm

3.5 Bcl-x is required for late embryonic cortical development.

To examine the role of Bcl-x in cortical development, histology was performed. Because cell death was not observed at early time points (E10- E12; data not shown), BKO tissue was examined at later embryonic time points for apoptotic cell death (E13-E19). At E13 a few apoptotic cells were observed in the cortex for the first time (Figure 3.5A). However, it was not until E17 that extensive apoptosis was observed in the cortex, specifically in the cortical plate. Apoptosis increased until E19 where it was widespread throughout the layers of the cortical plate but did not appear to affect cell populations of the VZ (Figure 3.5A). E19 cresyl violet stained tissue confirmed the location of condensed cell bodies throughout the upper layers of the cortical plate (Figure 3.5B). High magnification insets showed extensive apoptotic cell bodies throughout the cortex. Bcl-x therefore is required for survival of neurons in the upper cortical layers.

Figure 3.5: Onset of apoptotic cell death in the BKO cortex.

(A) Representative photomicrographs of E13, E17 and E19 coronal Ctl and BKO cortices labeled by active caspase-3 immunohistochemistry. A few apoptotic cells are observed in E13 BKO cortices, however, extensive apoptosis is not observed in the BKO cortex until E17. **(B)** Representative photomicrographs of coronal sections from E19 Ctl and BKO embryos stained with cresyl violet at low and high magnification. Arrows indicate condensed nuclei. D=dorsal, V=ventral, L=lateral, M=medial, A= apical, B= basal.

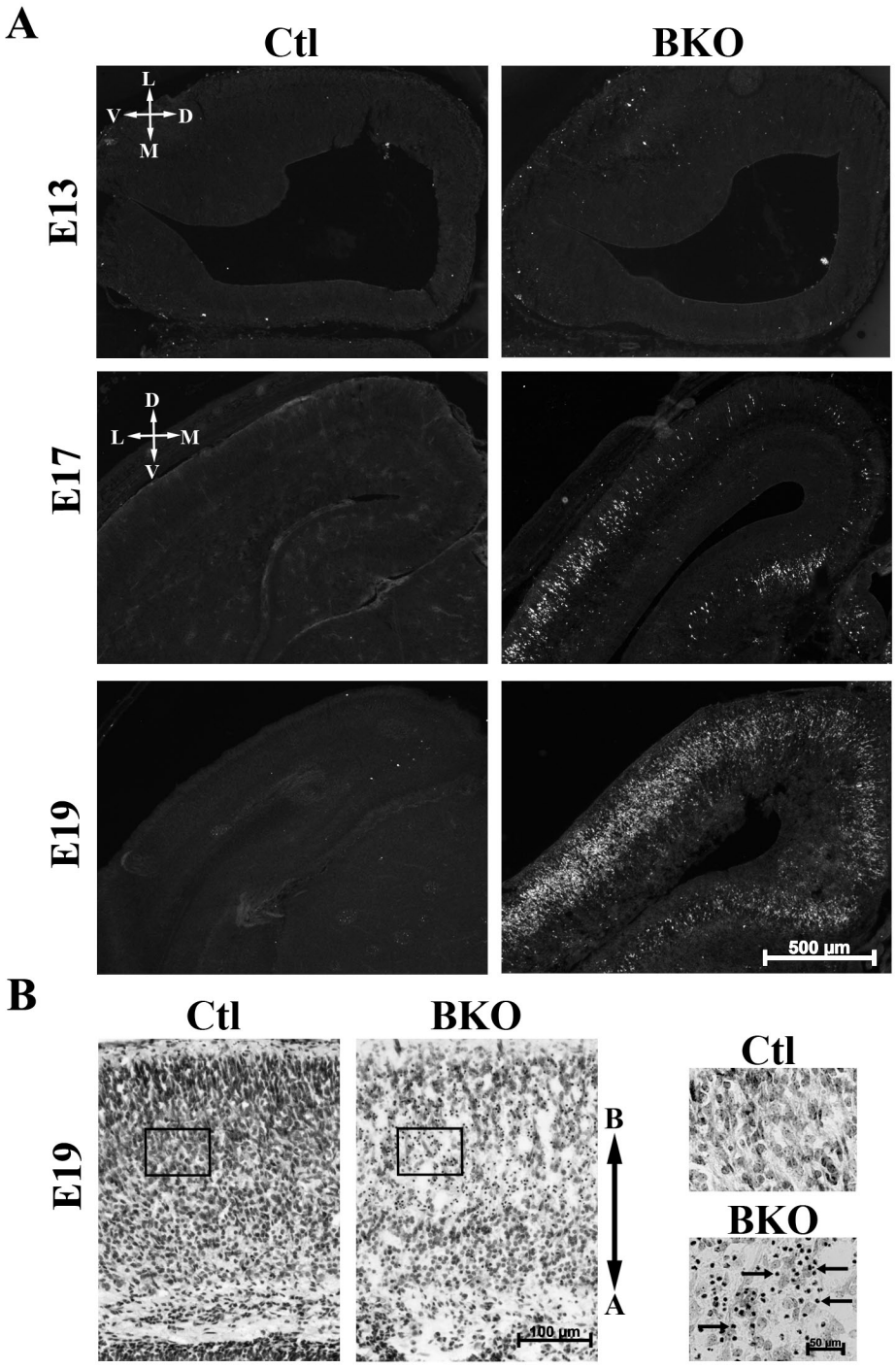
A
Ctl
BKO
E13
E17
E19
L
V
D
M
500 µm
B
Ctl
BKO
E19
B
A
100 µm
Ctl
BKO
50 µm

3.6 Proliferating population requires Mcl-1 but not Bcl-x for survival.

Given that the localization of cell death in MKO and BKO embryos overlapped with regions known to contain precursor populations in the ventricular zone of the forebrain and brainstem and around the midline of the spinal cord, apoptosis was examined in the proliferative precursor population. An intraperitoneal bromodeoxyuridine (BrdU) injection was given to pregnant dams 2 hours prior to sacrifice to label cells in S-phase of the cell cycle. At E13 BrdU-positive proliferating cells were seen primarily along the medial axis of the spinal cord with increased proliferative populations observed along the dorsal medial aspect of the spinal cord in embryos of all genotypes. At this time, the location of cell death in the spinal cords of MKO animals was widespread throughout the dorsal aspect with groups of apoptotic cells clustered together, while BKO embryos exhibited apoptosis throughout the ventral-lateral cellular populations. Immunohistochemistry for active caspase-3 and BrdU in coronal sections of E13 spinal cord revealed double labeling in MKO but not BKO animals (Figure 3.6). This suggests that Mcl-1 and not Bcl-x is required to maintain the survival of the proliferating populations.

Figure 3.6: Proliferating population requires Mcl-1 but not Bcl-x for survival. (A) Representative low magnification photomicrographs of coronal spinal cord sections from E13 Ctl, MKO and BKO animals labeled for active caspase-3 (green) and BrdU (pink). (B) High magnification photomicrographs of white boxed areas in A. Co-labeling of active caspase 3 and BrdU was observed in MKO tissue but not in Ctl or BKO tissue. Arrows point to double labeled cells.

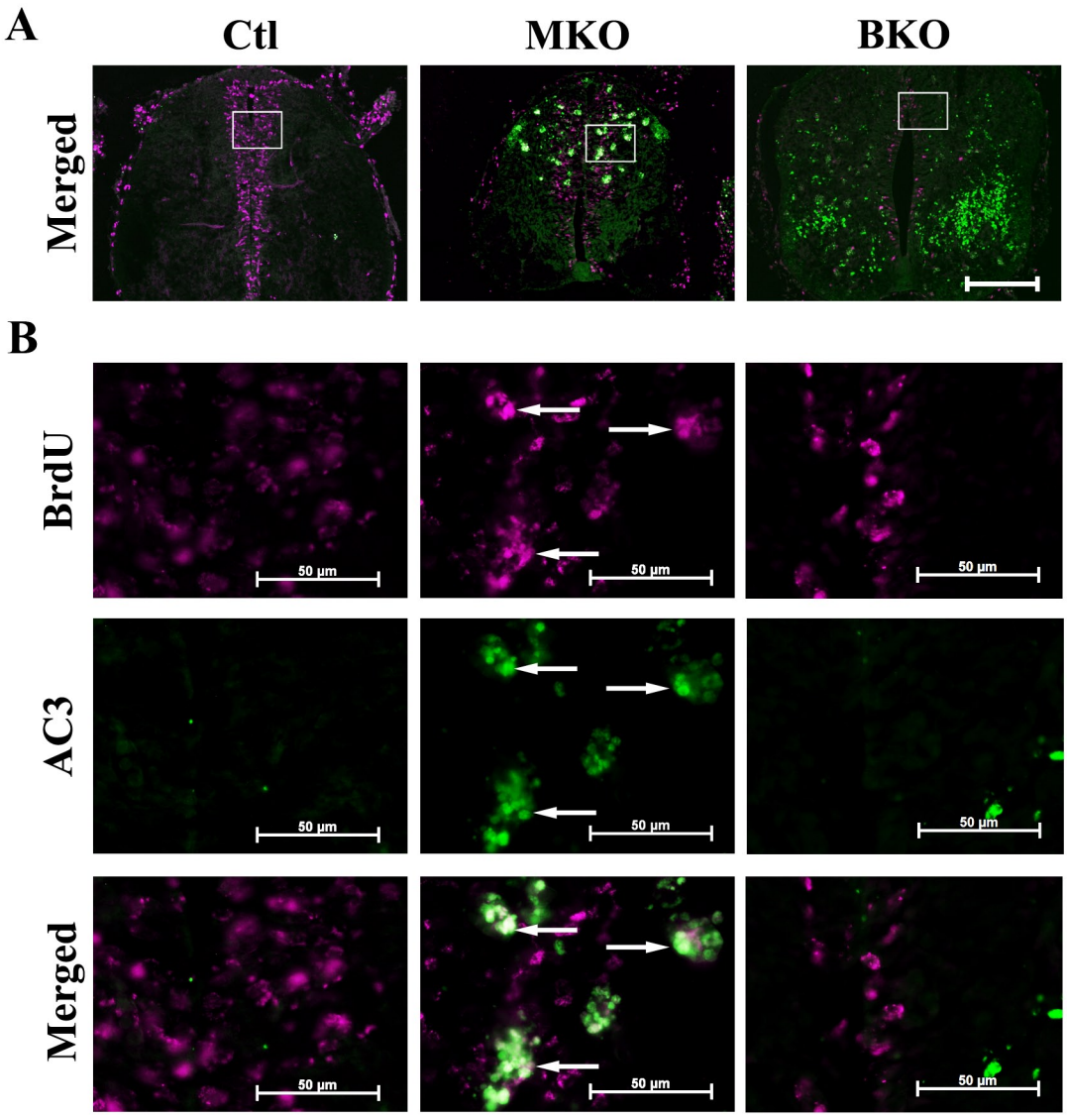
A
Ctl
MKO
BKO
Merged
B
BrdU
AC3
Merged
50 μm

3.7 Gene dosage effects on the onset of apoptosis.

Next, to determine whether Mcl-1 and Bcl-x have overlapping roles in CNS development, double knockout (DKO) embryos were generated. DKO animals for both *mcl-1* and *bcl-x* along with heterozygotes were used to examine gene dosage effects (Figures 3.7-3.9). Active caspase-3 immunohistochemistry and cresyl violet staining of E11 sagittal sections revealed the onset and extent of apoptosis throughout the spinal cord, brainstem and forebrain.

3.7.1 Spinal Cord

Sagittal spinal cord sections from double Het and Ctl animals revealed comparable levels of apoptosis (Figure 3.7). As shown previously, Mcl-1 and Bcl-x are required for survival in distinct populations as MKO embryos exhibit apoptosis along the dorsal aspect of the spinal cord at E11 while apoptosis was restricted to the ventral spinal cord in BKO embryos. In MKO:*bcl-x* Het embryos the pattern of apoptotic cell death was similar to that of the MKO at this time point, with extensive cell death restricted to the dorsal spinal cord. Although not quantified, there was consistently an observed increase in apoptotic cell death along the dorsal spinal cord in MKO:*bcl-x* Het embryos when compared with MKO littermates.

mcl-1 Het:BKO embryos exhibited cell death throughout the entire span of the spinal cord, unlike the single BKO animals, which had cell death largely

restricted to the ventral side. The loss of a single copy of *mcl-1* in BKO embryos did not appear to result in increased apoptosis throughout the post-mitotic population but did lead to vast cell death along the later developing dorsal spinal cord. The DKO displayed the most severe phenotype with widespread apoptosis spanning from ventral to dorsal throughout the entire spinal cord by E11.

Higher magnification photomicrographs confirmed the ventral/dorsal position of cell death throughout the various genotypes. Cresyl violet staining revealed healthy tissue in the spinal cords of control and double Het animals. Extensive condensed cell bodies were observed in the MKO, MKO:*bcl-x* Het and DKO high magnification cresyl violet-stained tissue sections, whereas scattered condensed cell bodies were seen in cresyl violet-stained sections of the BKO and *mcl-1* Het:BKO embryos. These results suggest that gene dosage does affect the amount and pattern of cell death throughout the E11 spinal cord.

Figure 3.7: Gene dosage affects the onset of apoptosis in the spinal cord.
Representative photomicrographs of sagittal spinal cord sections from E11 embryos of different genotypes as indicated (n= a minimum of 3/genotype). Apoptotic cells are labeled by active caspase-3 (AC3) immunohistochemistry while cresyl violet (CV) staining shows tissue histology. Larger boxed area indicates region of higher magnification photomicrographs for active caspase-3-stained sections, while smaller inset indicates region shown in cresyl violet photomicrographs. D= dorsal, V= ventral, R= rostral, C= caudal.

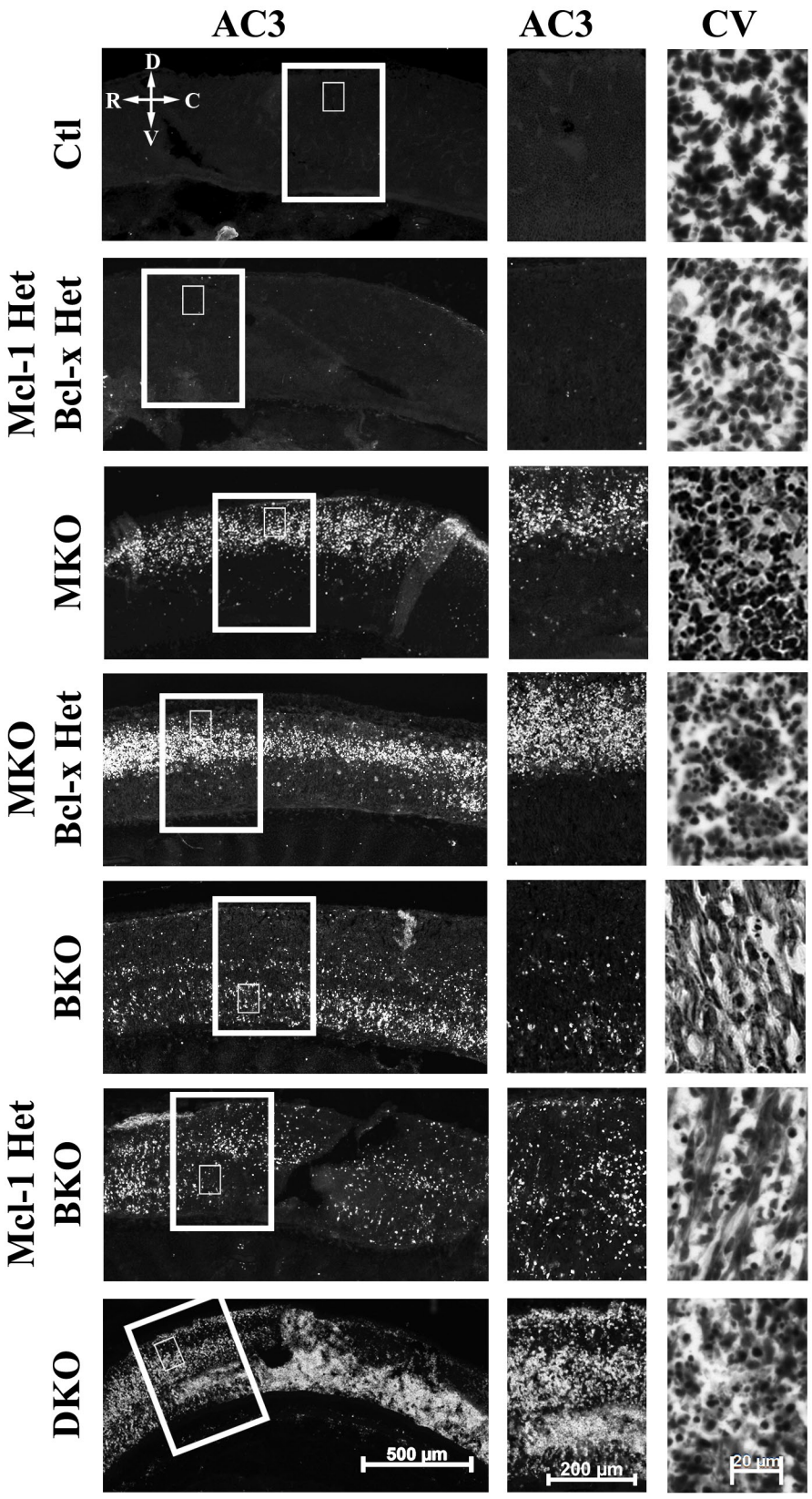
AC3
AC3
CV
Ctl
D
R
C
V
Mcl-1 Het
Bcl-x Het
MKO
MKO
Bcl-x Het
BKO
Mcl-1 Het
BKO
DKO
500 µm
200 µm
20 µm

3.7.2 Brainstem

To determine the effect of loss of both Mcl-1 and Bcl-x on the developing brainstem, tissue histology was performed on sagittal sections of E11 DKO and heterozygote embryos. As with the spinal cord, the level of cell death in the double heterozygote animals was comparable with controls (Figure 3.8). This was confirmed in cresyl violet-stained tissue where healthy cell morphology was observed.

In MKO:*bcl-x* Het embryos, apoptosis was observed around the ventricle similar to the pattern of cell death in MKO embryos. Higher magnification photomicrographs revealed that only cells within the VZ were affected. Although the same cell populations are affected in MKO and MKO:*bcl-x* Het embryos, there is more extensive apoptotic cell death throughout the VZ in MKO:*bcl-x* Het animals. Cresyl violet stained insets demonstrate condensed cell bodies throughout the ventricular region.

mcl-1 Het:BKO embryos had a unique phenotype with apoptotic cells spanning throughout the entire width of the brainstem. This was in contrast with BKO animals in which apoptosis was restricted to the basal region of post-mitotic cells. Although not quantified, it appears that the levels of apoptosis along the basal extent of the brainstem are comparable in both BKO and *mcl-1* Het: BKO embryos. This suggests that the loss of one copy of *mcl-1*, even in the absence of *bcl-x*, does not

further exaggerate the apoptotic phenotype in the basal post-mitotic cell population. This demonstrates unique roles for Mcl-1 and Bcl-x as well as their unique compensation capablities. Bcl-x is able to compensate to a limited extent for Mcl-1, whereas Mcl-1 does not appear to compensate for the loss of Bcl-x and plays a unique role solely in the VZ population. In magnified cresyl violet stained photomicrographs, both BKO and *mcl-1* Het:BKO tissue sections contain characteristic condensed cell bodies.

Finally, the brainstem was much smaller in the DKO with more extensive apoptotic cell death throughout the entire structure. The level of cell death appeared increased when compared with all other genotypes and vast amounts of condensed cell bodies were observed in cresyl violet stained sections. These results show a gene dosage effect in the combination of double knockout and heterozygote animals for *mcl-1* and *bcl-x*, similar to the pattern seen in the spinal cord.

Figure 3.8: Gene dosage affects the onset of apoptosis in the brainstem.
(A) Photomicrograph of cresyl violet stained E11 sagittal embryo. Black box indicates region of brainstem examined. **(B)** Representative photomicrographs of sagittal brainstem sections from embryos of different genotypes as indicated. Apoptotic cells are labeled by active caspase-3 (AC3) immunohistochemistry while cresyl violet staining shows tissue histology. Larger boxed area in left panels indicates region of higher magnification photomicrographs for active caspase-3 stained sections (middle), while smaller inset indicates region shown in cresyl violet (CV) photomicrographs (right). C= caudal, R= rostral, S= superior, I= inferior.

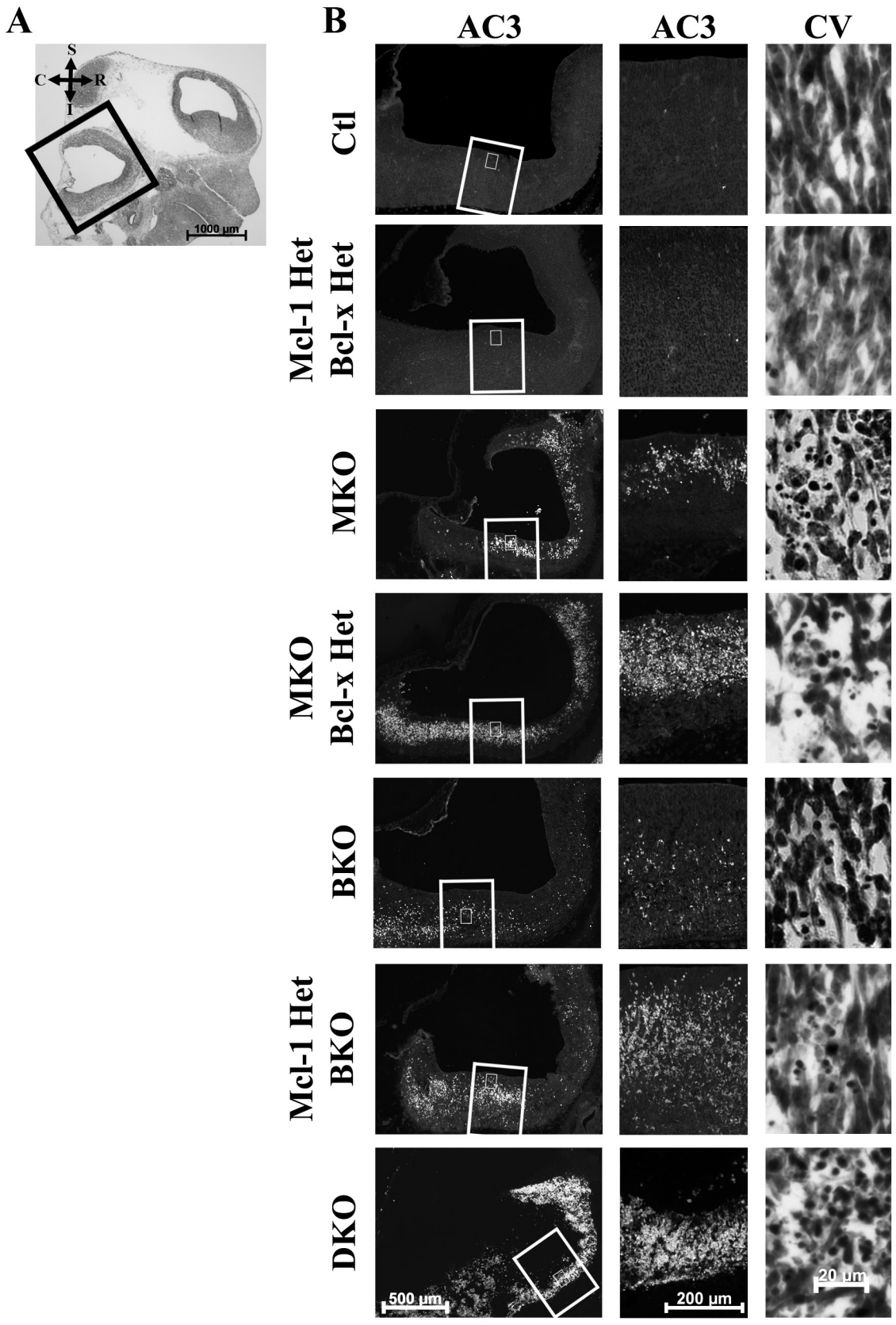
A
S
C
R
I
1000 µm
B
AC3
AC3
CV
Ctl
Mcl-1 Het
Bcl-x Het
MKO
MKO
Bcl-x Het
BKO
Mcl-1 Het
BKO
DKO
500 µm
200 µm
20 µm

3.7.3 Forebrain

No substantial cell death occurred in the forebrain of double heterozygote animals when compared with wild type Ctls (Figure 3.9). At E11 MKO embryos had extensive apoptotic cell death throughout the forebrain with the exception of the thalamus, which was spared. MKO:*bcl-x* Het embryos had a similar pattern, but had increased levels of apoptotic cell death widespread throughout the E11 forebrain when compared with MKO embryos. Apoptosis in these animals was throughout the width of the developing forebrain in all cell types as was seen in cresyl violet stained sections. BKO-only animals did not display any significant cell death throughout the forebrain at this time point. In contrast *mcl-1* Het:BKO embryos had minimal apoptosis in the pallium and subpallium. DKO embryos showed apoptotic cell death throughout the entire developing forebrain similar to what was seen in MKO:*bcl-x* Het animals. By E11 the width of the pallium in DKO embryos was dramatically reduced when compared with other genotypes including the MKO:*bcl-x* Het, as was seen in cresyl violet stained forebrain sections. Gene dosage does affect forebrain cell survival in the case of MKO:*bcl-x* Het and *mcl-1* Het:BKO animals, suggesting overlapping roles and possible compensation between Mcl-1 and Bcl-x.

Figure 3.9: Gene dosage affects the onset of apoptosis in the forebrain.
(A) Photomicrograph of cresyl violet stained E11 sagittal embryo. Black box indicates region of forebrain examined. **(B)** Representative photomicrographs of sagittal forebrain sections from embryos of different genotypes as indicated. Apoptotic cells are labeled by active caspase-3 (AC3) immunohistochemistry while cresyl violet (CV) staining shows tissue histology. Larger boxed area indicates region of higher magnification photomicrographs for active caspase-3 stained sections, while smaller inset indicates region shown in cresyl violet photomicrographs. R= rostral, C= caudal, B= basal, A= apical, S= superior, I= inferior.

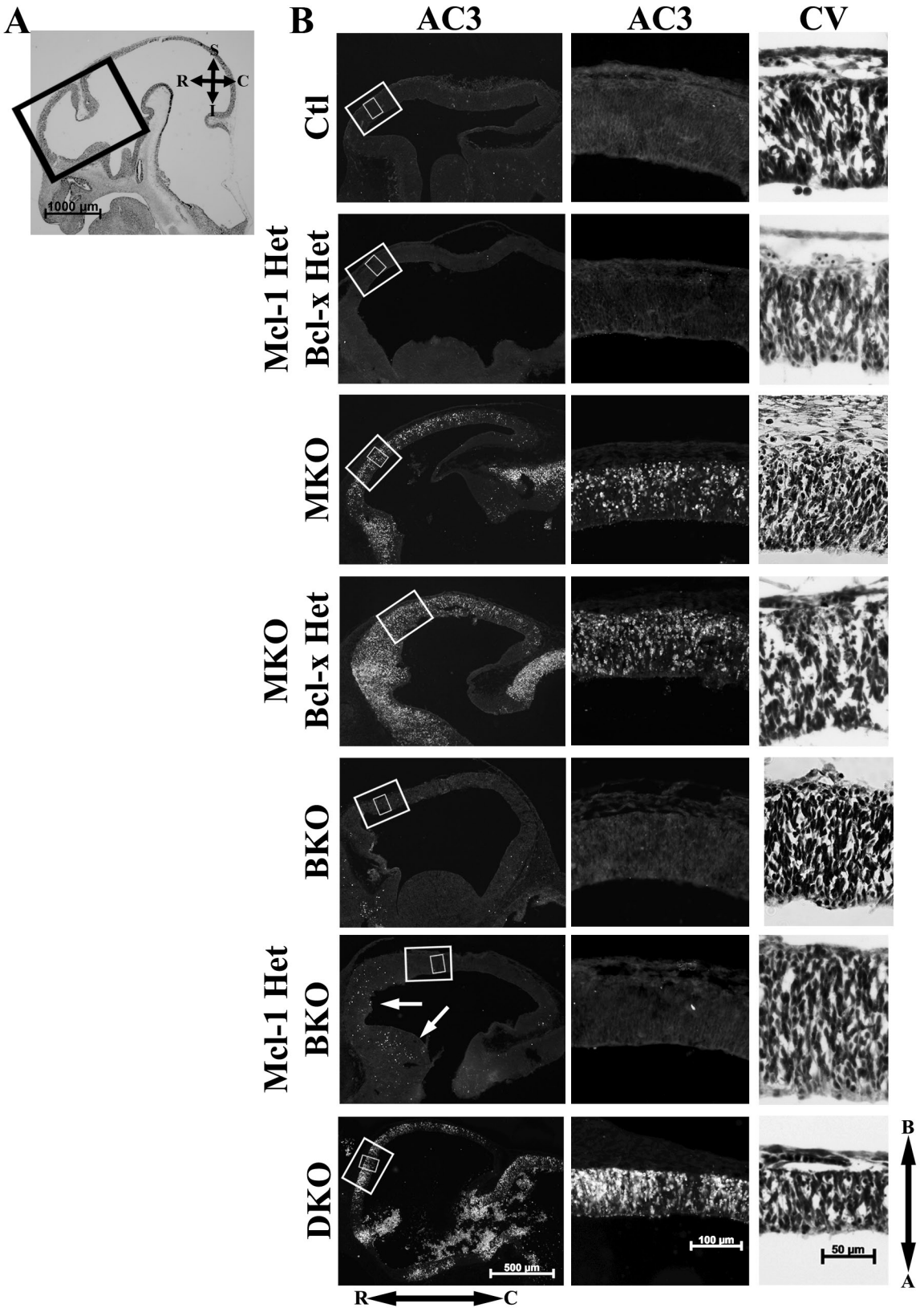
A
S
R
C
I
1000 µm
B
AC3
AC3
CV
Ctl
Mcl-1 Het
Bcl-x Het
MKO
MKO
Bcl-x Het
BKO
Mcl-1 Het
BKO
DKO
500 µm
100 µm
50 µm
R
C
B
A

3.8 Deletion of both *mcl-1* and *bcl-x* results in complete loss of the CNS by E14.

To determine the effect of *mcl-1* and *bcl-x* deletion on CNS development beyond E11, embryos were examined at E14. Cresyl violet staining was used to examine sagittal sections of E14 Ctl and DKO embryos. Low magnification photomicrographs revealed an empty cavity in the head and spinal column with loss of the entire CNS in DKO embryos (Figure 3.10A). Higher magnification photomicrographs of the cortex confirmed the loss of all neural tissue by this time point (Figure 3.10B). With the deletion of both *mcl-1* and *bcl-x*, all neuronal cell populations of the CNS undergo apoptosis.

Figure 3.10: Knockout of both *mcl-1* and *bcl-x* (DKO) results in complete loss of the CNS by E14.

(A) Representative photomicrographs of cresyl violet stained sagittal sections of Ctl and DKO whole embryos at E14. **(B)** High magnification photomicrographs of boxed areas of the forebrain stained with cresyl violet from Ctl and DKO embryos.

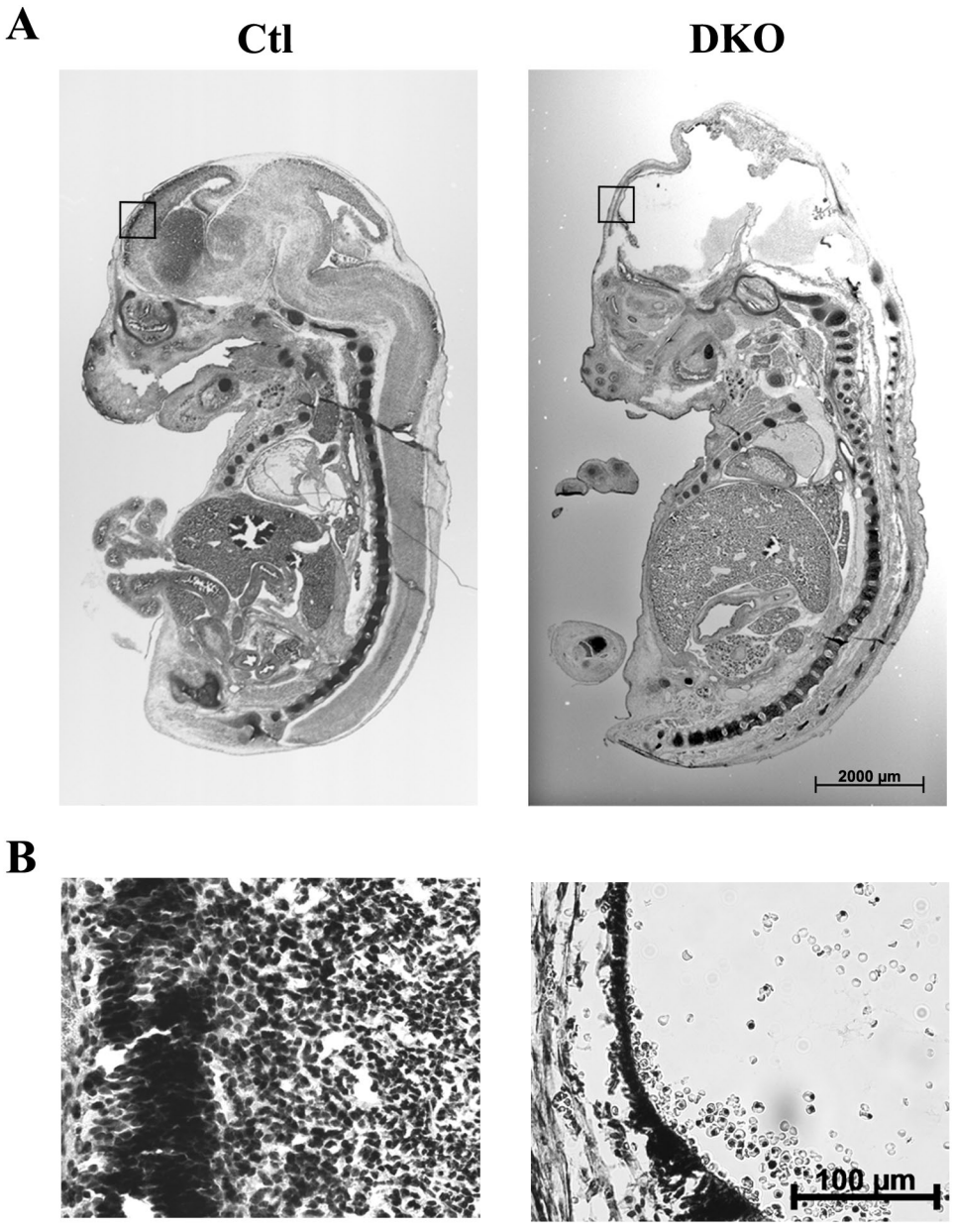
A
Ctl
DKO
2000 µm
B
100 µm

3.9 Deletion of *mcl-1*, *bcl-x* or both results in embryonic lethality.

Next, to determine whether the extent of cell death observed in the various knockout embryos resulted in embryonic lethality, embryonic survival was assessed at the following time points: E10, E11, E12, E13 and E14 for DKO embryos and E11, E13, E15, E17, E18 and E19 for BKO embryos. It has previously been established that the MKO model is embryonically lethal at E15.5 (Arbour et al. 2008). The BKO model, however, was found to be lethal at birth with expected Mendelian ratios collected at embryonic time points from E11 to birth (Table 3.1). DKO embryos were collected at expected Mendelian ratios or greater until E14, at which point there was a reduced number of DKO embryos collected compared to expected Mendelian ratios (Table 3.2). Later time points were not investigated for DKO animals given the known lethality at E15.5 for MKO embryos. These results suggest that the conditional deletion of *mcl-1*, *bcl-x* or both from the CNS results in lethality either throughout gestation or at the time of birth.

Table 3.1: Recovery of embryos from *bcl-x* mutants.

BKO	**Embryonic Time Point**						
	E11	**E13**	**E15**	**E17**	**E18**	**E19**	**Birth**
Number of litters	3	10	4	4	3	3	2
Total number of embryos	29	72	36	32	22	12	14
Number of knock-outs (%)	12 (41.3%)	19 (26.4%)	14 (38.9%)	6 (18.8%)	7 (31.8%)	1 (8.3%)	0 (0%)
Expected number Mendelian ratio (%)	5 (17.2%)	17.0 (23.6%)	7 (21.9%)	7 (21.9%)	5 (22.7%)	3 (25.0%)	3 (21.4%)

Table 3.2: Recovery of embryos from *mcl-1:bcl-x* mutants.

DKO	**Embryonic Time Point**				
	E10	**E11**	**E12**	**E13**	**E14**
Number of litters	5	4	2	2	2
Total number of embryos	44	32	17	16	20
Number of knock-outs (%)	5 (11.4%)	2 (6.3%)	1 (5.9%)	1 (6.3%)	1 (5.0%)
Expected number Mendelian ratio (%)	3 (6.8%)	2 (6.3%)	1 (5.9%)	1 (6.3%)	2 (10.0%)

3.10 Expression of pro-apoptotic *bcl-2* genes throughout the developing CNS.

Having demonstrated distinct and overlapping roles for Mcl-1 and Bcl-x, the expression of the pro-apoptotic *bcl-2* family genes were examined to determine those that were functionally responsible for the apoptotic cell death in the various knockout embryos. qRT-PCR was used to address which of the pro-apoptotic *bcl-2* genes were expressed in the forebrain, brainstem and spinal cord of the developing murine embryo. The expression of anti-apoptotic and pro-apoptotic *bcl-2* family members *mcl-1, bcl-x, bcl-w, bax, bak, bim, puma, noxa, bad, bid* and *bmf*, were examined at E10 and E12- time points prior to and following the onset of apoptosis. All genes investigated were transcibed at some level in the spinal cord, brainstem and forebrain of wild type embryos (Figure 3.11A, B, C). The expression of both *mcl-1* and *bcl-xL* increased from E10 to E12 in agreement with previous literature (Krajewska et al., 2002). *mcl-1* expression was approximately 2 to 3 fold greater than *bcl-xL*. This supports immunohistochemical data, which suggested Mcl-1 plays a greater role in survival earlier in development when there are a greater proportion of precursor cells.

A threshold level of expression was set at a RQ of 0.2 to identify pro-apoptotic genes expressed at the highest levels. This screening highlighted high levels of *bax, bak, bim, noxa* and *bmf* mRNA to be further examined for their expression patterns throughout the cell populations of the CNS.

Figure 3.11: Expression of apoptotic and anti-apoptotic *bcl-2* genes in the forebrain, brainstem and spinal cord.

Relative quantity (RQ) of gene expression in the **(A)** spinal cord, **(B)** brainstem and **(C)** forebrain from qRT-PCR completed on E10 (n=2) and E12 (n=3) tissue from wild type embryos. Gene expression is presented relative to *gapdh*. Red line indicates expression level threshold at which genes with greater expression were further examined. Fb=forebrain, Bs=brainstem and Sp=spinal cord. Results show mean+/- standard error of the mean (SEM).

A

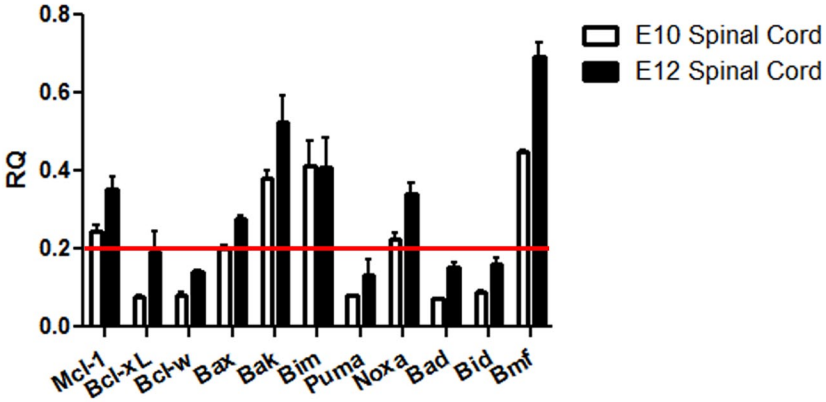
0.8
0.6
0.4
0.2
0.0
RQ
E10 Spinal Cord
E12 Spinal Cord
Mcl-1
Bcl-xL
Bcl-w
Bax
Bak
Bim
Puma
Noxa
Bad
Bid
Bmf

B

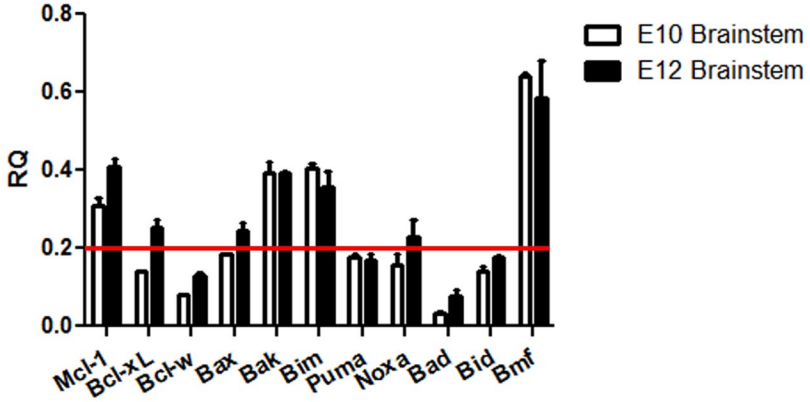
0.8
0.6
0.4
0.2
0.0
RQ
E10 Brainstem
E12 Brainstem
Mcl-1
Bcl-xL
Bcl-w
Bax
Bak
Bim
Puma
Noxa
Bad
Bid
Bmf

C

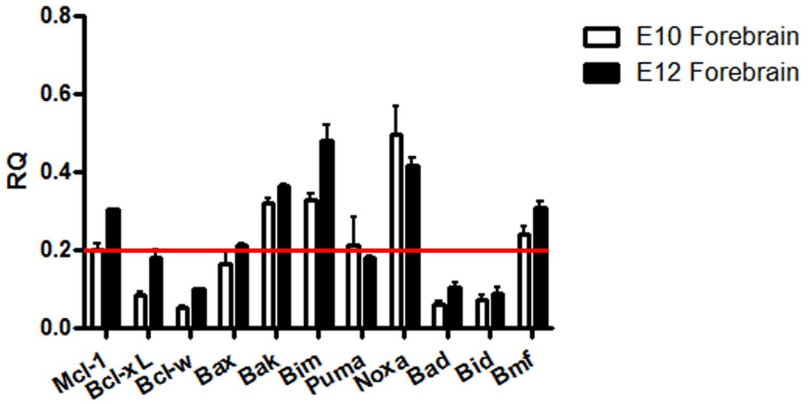
0.8
0.6
0.4
0.2
0.0
RQ
E10 Forebrain
E12 Forebrain
Mcl-1
Bcl-xL
Bcl-w
Bax
Bak
Bim
Puma
Noxa
Bad
Bid
Bmf

3.11 Expression of Bax, Noxa and Bmf are widespread throughout the early CNS.

To determine which cell populations within the CNS expressed the elevated pro-apoptotic *bcl-2* genes, *in situ* hybridization was performed on wild type embryos. At E13, expression of *bax, noxa* and *bmf* appeared widespread and diffuse throughout the entire CNS in sagittal sections from wild type C57BL/6 embryos (Figure 3.12A, B, C). Coronal forebrain and spinal cord sections from E11 wild type animals revealed a similar diffuse pattern of expression for *noxa*, but slightly more specific medial expression in the spinal cord for *bax* and *bmf*.

Figure 3.12: Expression of *bax, noxa* and *bmf* in the E13 CNS.

Representative photomicrographs of **(A)** *bax*, **(B)** *noxa* and **(C)** *bmf in situ* hybridization reveals diffuse expression throughout the CNS in sagittal sections from E13 as well as coronal sections of the forebrain and spinal cord from E11 wild type embryos. No staining was observed on the sense Ctl sections.

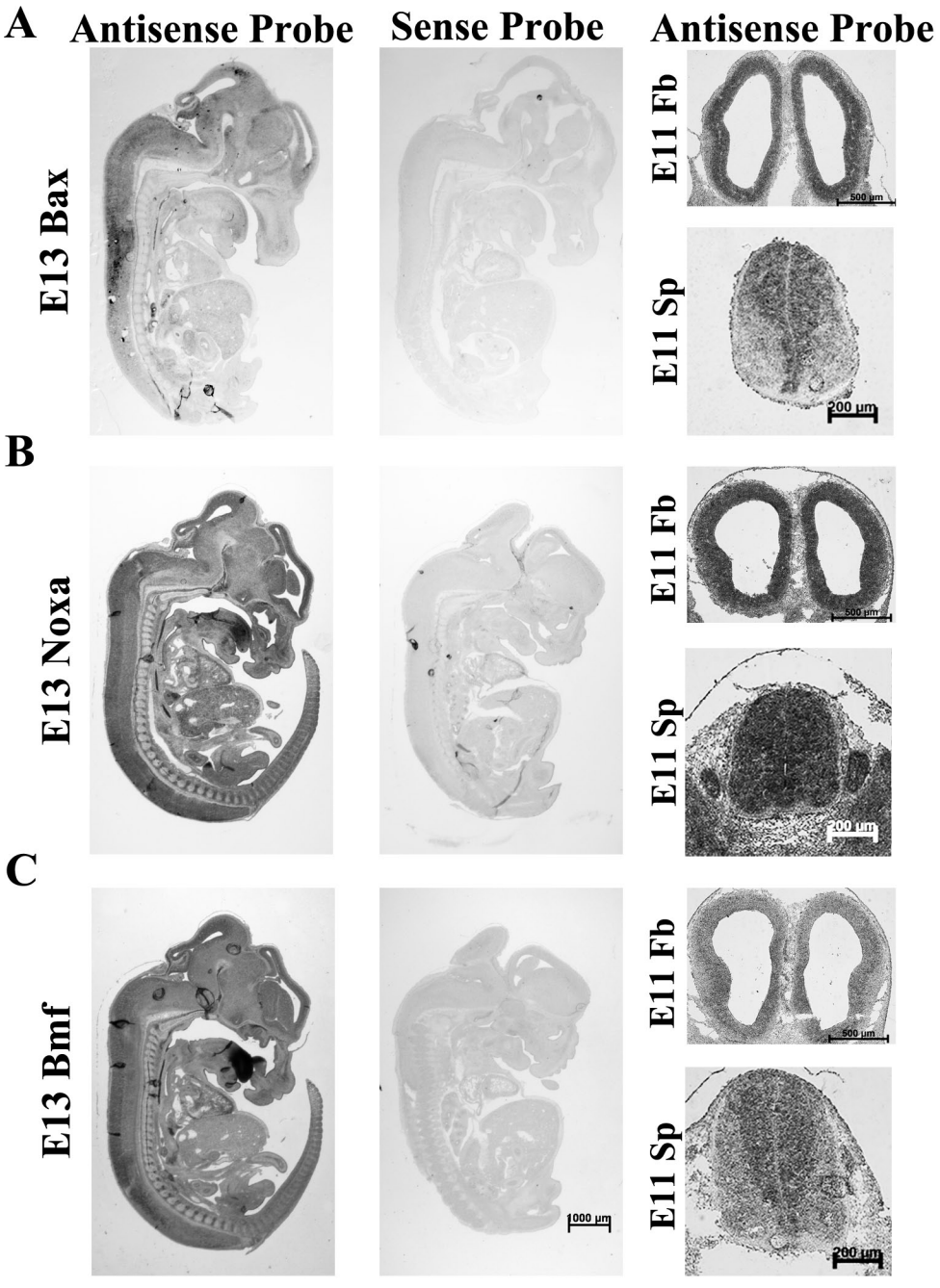
A
Antisense Probe
Sense Probe
Antisense Probe
E13 Bax
E11 Fb
E11 Sp
500 µm
200 µm
B
E13 Noxa
E11 Fb
E11 Sp
500 µm
200 µm
C
E13 Bmf
E11 Fb
E11 Sp
1000 µm
500 µm
200 µm

3.12 Expression of *bim* is restricted in the E13 CNS.

The specific expression pattern of *bim* throughout the developing CNS was investigated given that it was identified as a pro-apoptotic gene of elevated expression (Figure 3.11). To address this, *in situ* hybridization was performed on sagittal sections of E13 wild type C57BL/6 embryos. It was found that *bim* expression was restricted within the CNS (Figure 3.13A). Closer examination revealed highest expression throughout the entire E13 forebrain, the ventricular zone of the brainstem and the dorsal portion of the spinal cord (Figure 3.13B). Coronal E11 wild type tissue sections revealed restricted expression to the midline of the spinal cord and widespread expression in the early developing forebrain. The specificity of the expression of *bim* aligns with the pattern of apoptosis in E13 MKO: along the dorsal spinal cord, ventricular zone of the brainstem and throughout the forebrain. This could potentially explain the timing and pattern of cell death seen in MKO embryos, as Bim is known to interact with both Mcl-1 and Bcl-x.

Figure 3.13: Expression of *bim* in the E13 CNS.

(A) *In situ* hybridization reveals *bim* expression in sagittal sections from E13 Ctl embryos. No staining was observed on the sense Ctl sections. **(B)** Higher magnification photomicrographs of sagittal sections through the forebrain, brainstem and spinal cord of E13 Ctl embryos labeled with *bim* antisense probes. (**C**) Coronal sections through E11 forebrain and spinal cord, showing high *bim* expression within the proliferating regions in the Vz of the forebrain and around the central canal of the spinal cord. D= dorsal, V= ventral, R= rostral, C= caudal.

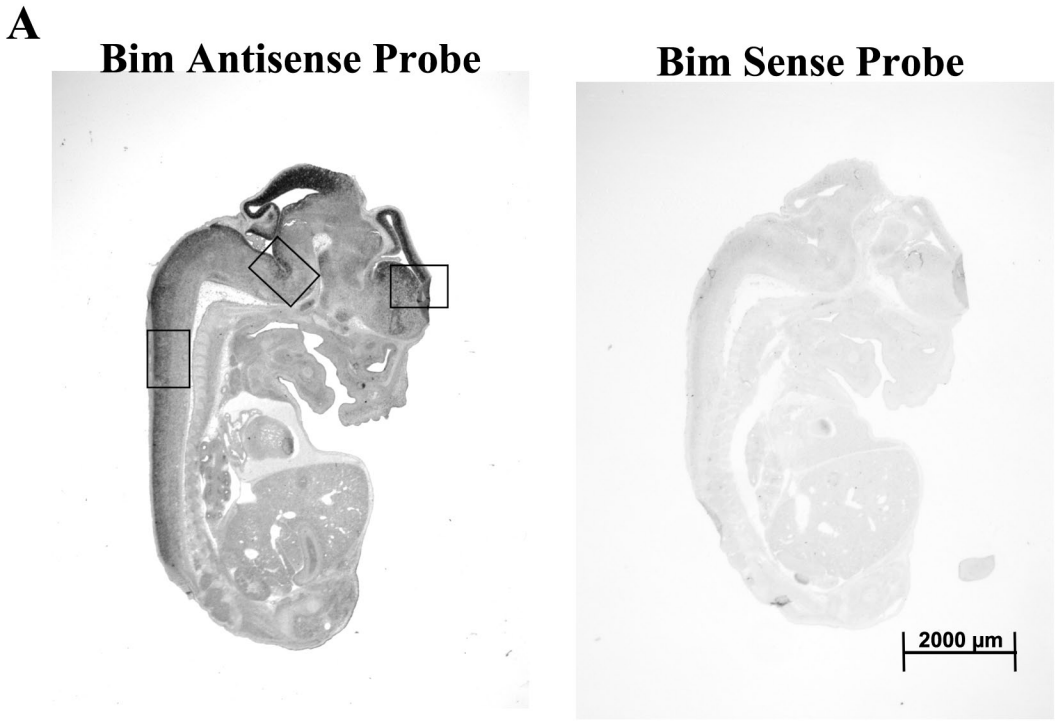
A
Bim Antisense Probe
Bim Sense Probe
2000 µm
B
Forebrain
Brainstem
Spinal Cord
E13
D
C
R
V
200 µm
C
Forebrain
Spinal Cord
E11
500 µm
200 µm

4.0 Discussion

This thesis has identified the roles of Mcl-1 and Bcl-x within the developing murine CNS using loss-of-function studies. First, it was demonstrated that the survival requirements for Mcl-1 and Bcl-x are distinct throughout the developing CNS with an earlier need for Mcl-1 than Bcl-x. Second, it was confirmed that Mcl-1 is required for precursor cell survival, while Bcl-x appears to play a role primarily in post-mitotic populations. Third, a DKO model revealed the compensatory role these two anti-apoptotic proteins perform for one another. Finally, elevated expression of five pro-apoptotic *bcl-2* family genes suggests that there may be key family members expressed within specific neural populations that preferentially interact with Mcl-1 or Bcl-x specifically. Taken together these results demonstrate the similar and distinct survival requirements for Mcl-1 and Bcl-x throughout CNS development.

4.1 Mcl-1 regulates precursor cell survival

Mcl-1 is a critical survival factor throughout neural precursor cell populations in the developing CNS. The onset of apoptosis throughout the CNS at early embryonic time points revealed the survival role of Mcl-1 throughout the proliferative populations. Previously, it has been shown in the forebrain that Mcl-1 is critical for survival as cells transition from precursors to post-mitotic neurons

(Arbour et al. 2008), this study however, was limited to the populations of the telencephalon. Here I have shown that the requirement for Mcl-1 is widespread in the precursor populations throughout the CNS. Although cell type-specific labeling was not verified, within the spinal cord, the survival requirement – as reflected by extensive apoptosis in the *mcl-1* loss-of-function, is observed first along the cells of the ventral aspect at E10. One day later the requirement for Mcl-1 is along the dorsal aspect of the spinal cord. The onset of neurogenesis within the spinal cord proceeds in a ventral-dorsal progression (McConnell 1981; Caspary & Anderson 2003). This demonstrates that as cells are transitioning from precursors to post mitotic neurons, they have a survival requirement for Mcl-1. The requirement for Mcl-1 as a pro-survival factor is widespread throughout the proliferative populations of the entire pre-natal CNS. In contrast the survival requirement for Bcl-x was apparent in populations at later time points through CNS development.

4.2 Bcl-x is essential for post-mitotic populations

Bcl-x is an essential survival factor for post-mitotic neurons throughout CNS development. In agreement with this, our study found later onset of apoptosis in BKO embryos, which suggests that it was the later developing neural populations that require Bcl-x for survival. Confirmation that Bcl-x was not required in the proliferative population reaffirmed the distinct need for Mcl-1 and not Bcl-x for

precursor cell survival. Previous studies have examined the role of Bcl-x in the developing CNS to a limited extent. In the germline *bcl-xL* knockout, only time points of E13 and younger were visually examined and the apoptotic cell death observed may have been confounded by the degradation of the hematopoietic system (Motoyama et al., 1995). Motoyama and colleagues (1995) found that there was cell death throughout the most developed regions of the CNS by E11.5 similar to my findings of the onset of apoptosis throughout the ventral spinal cord and brainstem but not in the forebrain. Roth and colleagues (1996) expanded the work of the *bcl-x* germline knockout and examined *in vitro* the survival of cortical progenitors from *bcl-x* KO mice. This work was also limited to a specific population of neurons – cortical neurons in the telencephalon and not necessarily representative of the entire CNS. In their study Roth and colleagues (1996) did find a significant cell death in the post-mitotic populations only. This result agrees with my findings of a later onset of apoptosis in the cortex at E17, at which point cell death is restricted to the post-mitotic populations of the cortical plate. Furthermore, using BrdU labeling I showed that at early developmental time points (E13) BKO embryos do not exhibit apoptosis within the proliferative populations of the spinal cord. Finally, a conditional KO model was generated that removed *bcl-x* from catecholaminergic populations (Savitt et al., 2005). This study resulted in a significant loss of these neurons but was again limited by a single cell population studied. Here, it has been demonstrated for the first time that throughout the entire CNS there is a prenatal requirement for Bcl-x in the post-mitotic neural populations. Furthermore

additional studies in our lab have shown that Bcl-x is an essential survival factor in specific post-mitotic neural populations. In addition to the requirement within catecholominergic neurons (Savitt et al. 2005), Bcl-x is also necessary for the survival of motor neurons within the spinal cord and facial motor nuclei of the brainstem, as well as Cux1-positive neurons of the cortex (unpublished data). Taken together these findings demonstrate the survival requirement for Bcl-x in prenatal post-mitotic neural populations.

Apoptosis of the motor neuron population in the spinal cord of BKO embryos occurs primarily from E11 to E13. This coincides with the peak period of motor neuron death in healthy developing murine embryos (Yamamoto & Henderson 1999). At this time motor neurons are primed for death and may be more susceptible to apoptosis resulting in population-specific losses seen in our BKO model. There are likely other post-mitotic neuronal populations unable to survive the deletion of *bcl-x* that we have yet to characterize. However, there are also many post-mitotic neurons that survive in this BKO model. Therefore, there must also be an alternative mechanism preventing the onset of apoptosis in the BKO CNS given the survival of Bcl-x-independent post-mitotic neuron populations.

4.3 Compensation of Bcl-x and Mcl-1

Mcl-1 and Bcl-x function cooperatively to maintain survival of cell populations during CNS development. It has been established here and through other studies that Mcl-1 is a critical survival factor throughout the precursor populations of the prenatal CNS while Bcl-x is critical to the survival of newly born post-mitotic neurons (Arbour et al. 2008; Savitt et al. 2005; Motoyama et al. 1995; Roth et al. 1996). However, loss of function of both Mcl-1 and Bcl-x demonstrated compensatory roles for both proteins. Cooperative function of Mcl-1 and Bcl-x has not been shown in the CNS before, expanding the previous understanding of CNS cell survival mechanisms. Mcl-1 and Bcl-x are known to function in a cooperative manner in other tissues including the development of megakaryocytes (Debrincat et al. 2012; Kodama et al. 2012), developing and adult hepatocytes (Hikita et al. 2009) as well as in pancreatic cancer cells (Takahashi et al. 2013). Results from this study demonstrate that Mcl-1 and Bcl-x function in a cooperative manner to maintain the survival of developing CNS cell populations.

A greater capacity for compensation of Bcl-x was apparent in patterns of apoptosis throughout MKO:*bcl-x* Het and *mcl-1* Het:BKO animals. Loss of one copy of the anti-apoptotic gene does not necessarily mean a 50% decrease in protein expression (Figure 3.1) as there are other mechanisms regulating expression. Similarly, it is unclear whether the loss of one *bcl-2* family gene affects the transcription or translation of the other. Preliminary results from our lab revealed

comparable expression of Bcl-x in Ctl, Mcl-1 Het and MKO embryos (data not shown) suggesting the loss of expression of one anti-apoptotic gene does not alter expression levels of another. Therefore, it is possible that any compensation between Mcl-1 and Bcl-x is a result of overlapping binding and neutralization capabilities of the pro-apoptotic family members with the levels of protein expressed under normal conditions within that cellular population. In the brainstem and spinal cord loss of one copy of *bcl-x* in MKO embryos resulted in a large increase in cell death indicating that Bcl-x does play a role in the survival of precursor populations. Similarly, the loss of one copy of *mcl-1* on a BKO background in the brainstem and spinal cord did appear to increase levels of apoptosis. However, unlike BKO animals where cell death remained along regions of post-mitotic cells, increased cell death in *mcl-1* Het:BKO embryos was predominantly in the precursor populations (Figure 4.1). This suggests that Mcl-1 does not play a large compensatory role in the survival of post-mitotic populations.

Survival mechanisms within the forebrain appeared different. Loss of Bcl-x seems to have little impact on forebrain cell survival from E11-E13 even with only one copy of Mcl-1. This was only examined in E11 embryos prior to the onset of neurogenesis in the rodent forebrain due to limitations of embryo survival past E11. In summary, my study suggests that Mcl-1 and Bcl-x have limited capabilities to compensate for one another throughout the developing murine CNS.

Figure 4.1: Compensation of Mcl-1 and Bcl-x through neurogenesis.

A summary figure demonstrates the early requirement for Mcl-1 (red gradient) with some compensation by Bcl-x (purple gradient). As the cell becomes post-mitotic, the requirement for survival seems to be Bcl-x, without any compensation from Mcl-1.

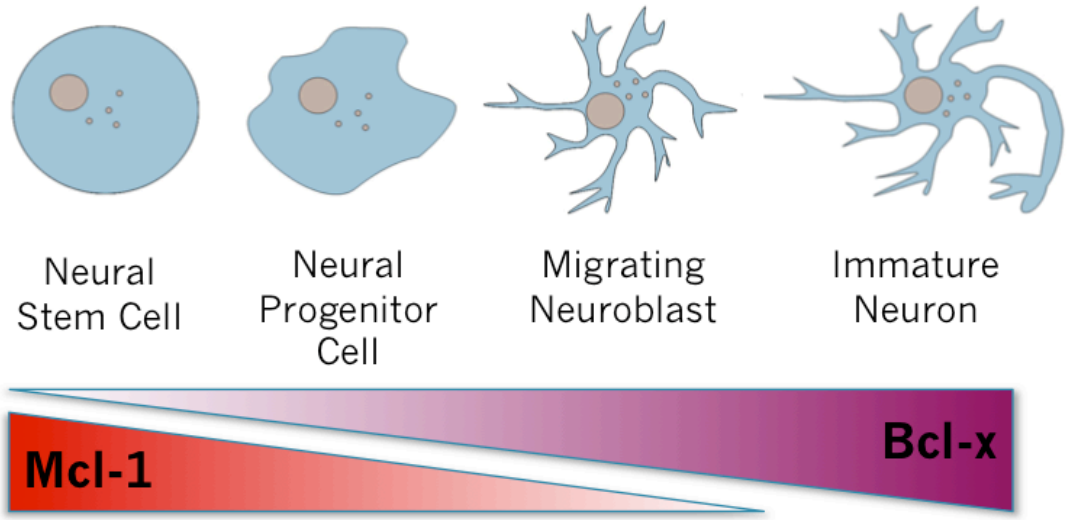
Neural Stem Cell
Neural Progenitor Cell
Migrating Neuroblast
Immature Neuron
Mcl-1
Bcl-x

4.4 Role of pro-apoptotic Bcl-2 proteins

Widespread expression of pro-apoptotic *bcl-2* family members suggests there may be many players at work regulating apoptosis in the developing CNS. Relatively high mRNA expression of five pro-apoptotic *bcl-2* family members under normal developmental conditions suggests in healthy cells there are multiple pro-apoptotic proteins whose activity is regulated by Mcl-1 and Bcl-x during CNS development. Previous literature suggests that Bad and Hrk will bind Bcl-x but not Mcl-1 and that Noxa will bind Mcl-1 but not Bcl-x (Moldoveanu et al. 2014). The remaining pro-apoptotic proteins are capable of being bound by both Mcl-1 and Bcl-x (Moldoveanu et al. 2014). Binding capabilities of Mcl-1 and Bcl-x as well as their proposed mechanisms of inhibition of pro-apoptotic Bcl-2 family members present numerous redundancies in their function (Czabotar et al. 2014). The unified model is the only current model that explains the range of results of Bcl-2 family interactions from previous literature. According to this model, both the BH3-only activators as well as the BH3-only sensitizers inhibit the anti-apoptotic proteins (Llambi et al. 2011). The anti-apoptotic proteins are also capable of inhibiting activated effector proteins as well as the BH3-only activators (Llambi et al. 2011). Of the five pro-apoptotic proteins with elevated expression during early neurogenesis, *in situ* hybridization pointed to restricted expression of *bim* throughout regions requiring Mcl-1 for survival, primarily precursor populations. Mcl-1 has previously

been demonstrated to have a greater binding affinity for Bim over the other BH3-only activators (Vela et al. 2013) and may be a viable target for rescue experiments in MKO animals. However, knockdown of Bim expression does not rescue the CNS abnormalities in Bcl-x deficient mice (Akhtar et al. 2008) and therefore there must be multiple pro-apoptotic proteins in addition to Bim regulating apoptosis in DKO embryos. Further downstream effector proteins Bax and Bak also demonstrated elevated expression and are essential for the propagation of the apoptotic signal. Willis and colleagues (2005) demonstrated that Bak is sequestered solely by Mcl-1 and Bcl-x and not by Bcl-2, Bcl-w or A1. It is possible that the mechanism of apoptosis in certain populations is driven primarily by Bak with the loss of function of both Mcl-1 and Bcl-x. Previously known interactions of Bcl-2 family proteins as well as elevated expression of 5 pro-apoptotic proteins suggest that there are multiple activator and effector proteins acting to regulate apoptosis throughout neural development.

4.5 Future Studies

It is clear that Mcl-1 and Bcl-x are the two major anti-apoptotic Bcl-2 family proteins regulating cell survival of the developing CNS. Despite the high levels of mRNA expression of 5 pro-apoptotic family members, the mechanism of apoptosis in MKO and BKO embryos was not fully elucidated through this study. Western blotting or immunohistochemistry would confirm if pro-apoptotic protein

expression levels were consistent with mRNA expression patterns. Given the cell population-specific requirements as well as the complexities of interactions between Bcl-2 family members, *in vitro* examination of a number of cell types may provide a clear indication of the pro-apoptotic proteins functionally responsible for the elevated levels of apoptosis with the loss-of-function of either Mcl-1 or Bcl-x. RNAi techniques would also help clarify pro-apoptotic Bcl-2 family members regulating apoptosis throughout the developing CNS through knockdown of individual targets. Initially the role of the effector proteins Bax and Bak in apoptotic cell death within MKO and BKO should be identified. Loss of both Bax and Bak should block all apoptosis initiated via the Bcl-2 family and has been shown to rescue the phenotype in Mcl-1 and Bcl-x deficient megakaryocytic lineages (Kodama et al. 2012). Additionally BH3-only activator Bim appears to be a promising target for the rescue of the MKO apoptotic phenotype. Further study is warranted to demonstrate the complete mechanism regulating survival in the developing neural populations.

The level of protein expression in KO and Het animals is not entirely clear. We do not suspect that the loss of one protein impacts the expression of the other based on examination of western blots from single MKO or BKO animals. However, quantification of the expression in KO:Het animals would further elucidate the compensatory capabilities between these two proteins.

Complete apoptotic cell death occurs very early in the developing DKO CNS. It is likely that all cells undergo apoptosis as precursors in DKO embryos, and

therefore whether post-mitotic neurons would be capable of survival without Bcl-x and Mcl-1 remains to be shown. It is possible that additional anti-apoptotic Bcl-2 family proteins contribute to the survival of post-mitotic neural populations. *In vitro* experiments or loss of function studies using a cre expressing plasmid electroporated *in utero* at a later developmental time point could be used to selectively knockout *mcl-1* and *bcl-xL* in a specific post mitotic neuronal population. This would clarify if post mitotic neurons are capable of survival with the loss of both Mcl-1 and Bcl-x and if there is any additional compensation from other anti-apoptotic Bcl-x proteins in the post-mitotic population.

4.6 Conclusion

Here, I have examined the role of anti-apoptotic Bcl-2 proteins, Mcl-1 and Bcl-x, in promoting survival as cells progress through neurogenesis. Extensive apoptotic cell death in the forebrain, brainstem and spinal cord of CKO models demonstrate that Mcl-1 is crucial for precursor cell survival and Bcl-x is critical for the survival of post-mitotic neural populations. DKO embryos exhibit a more severe phenotype than either MKO or BKO embryos with complete loss of the CNS by E14. This demonstrates a compensatory role between Mcl-1 and Bcl-x. Examination of pro-apoptotic *bcl-2* family members point to five genes (*bim*, bmf, noxa, bax, bak) with elevated expression throughout CNS development that should be further investigated to determine their role in CNS cell survival regulation. This study

demonstrates for the first time the distinct and compensatory requirements for Mcl-1 and Bcl-x within the developing murine CNS.

5.0 Bibliography

Akhtar, R.S. et al., 2008. Loss of BH3-only protein Bim inhibits apoptosis of hemopoietic cells in the fetal liver and male germ cells but not neuronal cells in bcl-x-deficient mice. *The Journal of Histochemistry and Cytochemistry : Official Journal of the Histochemistry Society*, 56(10), pp.921–927.

Angevine, J.B. & Sidman, R.L., 1961. Autoradiographic study of cell migration during histogenesis of cerebral cortex in the mouse. *Nature*, 192, pp.766–768.

Arbour, N. et al., 2008. Mcl-1 is a key regulator of apoptosis during CNS development and after DNA damage. *The Journal of Neuroscience : The Official Journal of the Society for Neuroscience*, 28(24), pp.6068–78.

Boatright, K.M. & Salvesen, G.S., 2003. Mechanisms of caspase activation. *Current Opinion in Cell Biology*, 15(6), pp.725–731.

Boise, L.H. et al., 1993. Bcl-X, a Bcl-2-related gene that functions as a dominant regulator of apoptotic cell death. *Cell*, 74(4), pp.597–608.

Briscoe, J. & Ericson, J., 2001. Specification of neuronal fates in the ventral neural tube. *Current Opinion in Neurobiology*, 11(1), pp.43–49.

Bursch, W., Kleine, L. & Tenniswood, M, 1990. The biochemistry of cell death by apoptosis. *Biochemistry and Cell Biology*, 68, 1071–1074.

Caspary, T. & Anderson, K. V, 2003. Patterning cell types in the dorsal spinal cord: what the mouse mutants say. *Nature Reviews. Neuroscience*, 4(4), pp.289–97.

Chen, L. et al., 2005. Differential targeting of prosurvival Bcl-2 proteins by their BH3-only ligands allows complementary apoptotic function. *Molecular Cell*, 17(3), pp.393–403.

Chen, S.C., Curran, T., & Morgan, J.I., 1995. Apoptosis in the nervous system: new revelations. *Journal of Clinical Pathology*, 48(1), pp.7–12.

Chipuk, J.E. et al., 2010. The BCL-2 family reunion. *Molecular Cell*, 37(3), pp.299–310.

Cuconati, A. & Mukherjee, C., 2003. DNA damage response and MCL-1 destruction initiate apoptosis in adenovirus-infected cells. *Genes and Development*, 17(23), pp.2922–2932.

Czabotar, P.E. et al., 2014. Control of apoptosis by the BCL-2 protein family: implications for physiology and therapy. *Nature Reviews. Molecular Cell Biology*, 15(1), pp.49–63.

Debrincat, M. a et al., 2012. Mcl-1 and Bcl-x(L) coordinately regulate megakaryocyte survival. *Blood*, 119(24), pp.5850–8.

Dutta, S. et al., 2010. Determinants of BH3 binding specificity for Mcl-1 versus Bcl-xL. *Journal of Molecular Biology*, 398(5), pp.747–62.

Dzhagalov, I., Dunkle, a. & He, Y.-W., 2008. The anti-apoptotic Bcl-2 family member Mcl-1 promotes T lymphocyte survival at multiple stages. *The Journal of Immunology*, 181(1), pp.521–528.

Dzhagalov, I., John, A. & He, Y., 2007. The antiapoptotic protein Mcl-1 is essential for the survival of neutrophils but not macrophages. *Blood*, 109(4), pp.1620–1626.

Fan, T.-J. et al., 2005. Caspase family proteases and apoptosis. *Acta Biochimica et Biophysica Sinica*, 37(11), pp.719–727.

Fietz, S. a & Huttner, W.B., 2011. Cortical progenitor expansion, self-renewal and neurogenesis-a polarized perspective. *Current Opinion in Neurobiology*, 21(1), pp.23–35.

Gao, J. et al., 2010. IRF-1 transcriptionally upregulates PUMA, which mediates the mitochondrial apoptotic pathway in IRF-1-induced apoptosis in cancer cells. *Cell Death and Differentiation*, 17(4), pp.699–709.

Götz, M. & Huttner, W.B., 2005. The cell biology of neurogenesis. *Nature Reviews. Molecular Cell Biology*, 6(10), pp.777–788.

Grad, J.M., Zeng, X.R. & Boise, L.H., 2000. Regulation of Bcl-xL: a little bit of this and a little bit of STAT. *Current Opinion in Oncology*, 12(6), pp.543–9.

Green, D.R., 2000. Apoptotic pathways: paper wraps stone blunts scissors. *Cell*, 102(1), pp.1–4.

Hamasaki, A. et al., 1998. Accelerated neutrophil apoptosis in mice lacking A1-a, a subtype of the bcl-2-related A1 gene. *The Journal of Experimental Medicine*, 188(11), pp.1985–1992.

Harder, J.M. et al., 2012. BCL2L1 (BCL-X) promotes survival of adult and developing retinal ganglion cells. *Molecular and Cellular Neurosciences*, 51(1-2), pp.53–9.

Hasan, S.M.M. et al., 2013. Mcl1 regulates the terminal mitosis of neural precursor cells in the mammalian brain through p27Kip1. *Development*, 140(15), pp.3118–27.

Haubensak, W. et al., 2004. Neurons arise in the basal neuroepithelium of the early mammalian telencephalon: a major site of neurogenesis. *Proceedings of the National Academy of Sciences of the United States of America*, 101(9), pp.3196–201.

Hikita, H. et al., 2009. Mcl-1 and Bcl-xL cooperatively maintain integrity of hepatocytes in developing and adult murine liver. *Hepatology*, 50(4), pp.1217–1226.

Hotchkiss, R. et al., 2009. Cell Death. *New England Journal of Medicine*, 361(16), pp.1570–83.

Jessell, T.M., 2000. Neuronal specification in the spinal cord: inductive signals and transcriptional codes. *Nature Reviews. Genetics*, 1(1), pp.20–9.

Kerr, J., Wyllie, A. & Currie, A., 1972. Apoptosis: A basic biological phenomenon with wide-ranging implications in tissue kinetics. *British Journal of Cancer*.

Kodama, T. et al., 2012. Mcl-1 and Bcl-xL regulate Bak/Bax-dependent apoptosis of the megakaryocytic lineage at multistages. *Cell Death and Differentiation*, 19(11), pp.1856–69.

Kozopas, K.M. et al., 1993. MCL1, a gene expressed in programmed myeloid cell differentiation, has sequence similarity to BCL2. *Proceedings of the National Academy of Sciences of the United States of America*, 90(8), pp.3516–20.

Krajewska, M. et al., 2002. Dynamics of expression of apoptosis-regulatory proteins Bid, Bcl-2, Bcl-X, Bax and Bak during development of murine nervous system. *Cell Death and Differentiation*, 9(2), pp.145–157.

Kristiansen, M. & Ham, J., 2014. Programmed cell death during neuronal development: the sympathetic neuron model. *Cell Death and Differentiation*, 21(7), pp.1025–35.

Kuwana, T. et al., 2005. BH3 domains of BH3-only proteins differentially regulate Bax-mediated mitochondrial membrane permeabilization both directly and indirectly. *Molecular Cell*, 17(4), pp.525–535.

Kuwana, T. et al., 2002. Bid, Bax, and lipids cooperate to form supramolecular openings in the outer mitochondrial membrane. *Cell*, 111(3), pp.331–342.

Letai, A. et al., 2002. Distinct BH3 domains either sensitize or activate mitochondrial apoptosis, serving as prototype cancer therapeutics. *Cancer Cell*, 2(3), pp.183–92.

Llambi, F. et al., 2011. A unified model of mammalian BCL-2 protein family interactions at the mitochondria. *Molecular Cell*, 44(4), pp.517–31.

Lomonosova, E. & Chinnadurai, G., 2008. BH3-only proteins in apoptosis and beyond: an overview. *Oncogene*, 27 Suppl 1(S1), pp.S2–19.

Malone, C.D. et al., 2012. Mcl-1 regulates the survival of adult neural precursor cells. *Molecular and Cellular Neurosciences*, 49(4), pp.439–47.

McConnell, J. a, 1981. Identification of early neurons in the brainstem and spinal cord. II. An autoradiographic study in the mouse. *The Journal of Comparative Neurology*, 200(2), pp.273–88.

Metcalfe, A.D. et al., 2004. Expression of 11 members of the BCL-2 family of apoptosis regulatory molecules during human preimplantation embryo development and fragmentation. *Molecular Reproduction and Development*, 68(1), pp.35–50.

Michaelidis, T.M. et al., 1996. Inactivation of bcl-2 results in progressive degeneration of motoneurons, sympathetic and sensory neurons during early postnatal development. *Neuron*, 17(1), pp.75–89.

Moldoveanu, T. et al., 2014. Many players in BCL-2 family affairs. *Trends in Biochemical Sciences*, 39(3), pp.101–111.

Molnár, Z., 2011. Evolution of cerebral cortical development. *Brain, Behavior and Evolution*, 78(1), pp.94–107.

Molnár, Z., Vasistha, N. a & Garcia-Moreno, F., 2011. Hanging by the tail: progenitor populations proliferate. *Nature Neuroscience*, 14(5), pp.538–40.

Motoyama, N. et al., 1995. Massive cell death of immature hematopoietic cells and neurons in Bcl-x-deficient mice. *Science*, 267(5203), pp.1506–10.

Nijhawan, D., Honarpour, N. & Wang, X., 2000. Apoptosis in neural development and disease. *Annual Review of Neuroscience*, 23, pp.73–87.

Nornes, H. & Carry, M., 1978. Neurogenesis in spinal cord of mouse: an autoradiographic analysis. *Brain Research*, 159, pp.1–16.

Ola, M.S., Nawaz, M. & Ahsan, H., 2011. Role of Bcl-2 family proteins and caspases in the regulation of apoptosis. *Molecular and Cellular Biochemistry*, 351(1-2), pp.41–58.

Opferman, J.T. et al., 2003. Development and maintenance of B and T lymphocytes requires antiapoptotic MCL-1. *Nature*, 426(6867), pp.671–676.

Opferman, J.T. et al., 2005. Obligate role of anti-apoptotic MCL-1 in the survival of hematopoietic stem cells. *Science*, 307(5712), pp.1101–4.

Oppenheim, R.W., 1991. Cell death during development of the nervous system. *Annual Review of Neuroscience*, 14, pp.453–501.

Oppenheim, R.W., 1981. Cell death of motoneurons in the chick embryo spinal cord. V. Evidence on the role of cell death and neuromuscular function in the formation of specific peripheral connections. *The Journal of Neuroscience : The Official Journal of the Society for Neuroscience*, 1(2), pp.141–151.

Peng, R. et al., 2013. Targeting Bax interaction sites reveals that only homo-oligomerization sites are essential for its activation. *Cell Death and Differentiation*, 20(5), pp.744–54.

Print, C.G. et al., 1998. Apoptosis regulator Bcl-w is essential for spermatogenesis but appears otherwise redundant. *Proceedings of the National Academy of Sciences of the United States of America*, 95(21), pp.12424–12431.

Rinkenberger, J.L. et al., 2000. Mcl-1 deficiency results in peri-implantation embryonic lethality. *Genes and Development*, 14(1), pp.23–27.

Ross, A.J. et al., 1998. Testicular degeneration in Bclw-deficient mice. *Nature Genetics*, 18(3), pp.251–256.

Roth, K. a et al., 2000. Epistatic and independent functions of caspase-3 and Bcl-X(L) in developmental programmed cell death. *Proceedings of the National Academy of Sciences of the United States of America*, 97(1), pp.466–71.

Roth, K. & D'Sa, C., 2001. Apoptosis and brain development. *Mental Retardation and Developmental Disabilities Research Reviews*, 7(4), pp.261–266.

Roth, K., Motoyama, N. & Loh, D., 1996. Apoptosis of bcl-x-deficient telencephalic cells in vitro. *The Journal of Neuroscience*, 76(5).

Rucker, E.B. et al., 2000. Bcl-x and Bax regulate mouse primordial germ cell survival and apoptosis during embryogenesis. *Molecular Endocrinology*, 14(7), pp.1038–52.

Sauer, B., 1998. Inducible gene targeting in mice using the Cre/lox system. *Methods*, 14(4), pp.381–92.

Savill, J. & Fadok, V., 2000. Corpse clearance defines the meaning of cell death. *Nature*, 407(6805), pp.784–788.

Savitt, J.M. et al., 2005. Bcl-x is required for proper development of the mouse substantia nigra. *The Journal of Neuroscience : the Official Journal of the Society for Neuroscience*, 25(29), pp.6721–8.

Schellenberg, B. et al., 2013. Article Bax exists in a dynamic equilibrium between the cytosol and mitochondria to control apoptotic priming. *Molecular Cell*, 49(5), pp.959–971.

Shamas-Din, A. et al., 2013. Mechanisms of action of Bcl-2 family proteins. *Cold Spring Harbor Perspectives in Biology*, 5(4), p.a008714.

Sims, T.J. & Vaughn, J.E., 1979. The generation of neurons involved in an early reflex pathway of embryonic mouse spinal cord. *The Journal of Comparative Neurology*, 183(4), pp.707–19.

Steimer, D., Boyd, K. & Takeuchi, O., 2009. Selective roles for antiapoptotic MCL-1 during granulocyte development and macrophage effector function. *Blood*, 113(12), pp.2805–2815.

Takahashi, H., Chen, M. & Pham, H., 2013. Simultaneous knock-down of Bcl-xL and Mcl-1 induces apoptosis through Bax activation in pancreatic cancer cells. *Biochimica et Biophysica Acta*, 1833(12), pp.2980–2987.

Thornberry, N.A. & Lazebnik, Y., 1998. Caspases: enemies within. *Science*, 281(5381), pp.1312–1316.

Uren, R.T. et al., 2007. Mitochondrial permeabilization relies on BH3 ligands engaging multiple prosurvival Bcl-2 relatives, not Bak. *Journal of Cell Biology*, 177(2), pp.277–287.

Vaux, D.L., Cory, S. & Adams, J.M., 1988. Bcl-2 gene promotes haemopoietic cell survival and cooperates with c-myc to immortalize pre-B cells. *Nature*, 335(6189), pp.440–442.

Vela, L. et al., 2013. Direct interaction of Bax and Bak proteins with Bcl-2 homology domain 3 (BH3)-only proteins in living cells revealed by fluorescence complementation. *The Journal of Biological Chemistry*, 288(7), pp.4935–46.

Vikstrom, I. et al., 2010. Mcl-1 is essential for germinal center formation and B cell memory. *Science*, 330(6007), pp.1095–9.

Wang, X., Bathina, M. & Lynch, J., 2013. Deletion of MCL-1 causes lethal cardiac failure and mitochondrial dysfunction. *Genes and Development*, 3, pp.1351–1364.

Wei, M.C. et al., 2000. tBID, a membrane-targeted death ligand, oligomerizes BAK to release cytochrome c. *Genes and Development*, 14(16), pp.2060–2071.

White, L.D. & Barone, S. 2001. Qualitative and quantitative estimates of apoptosis from birth to senescence in the rat brain. *Cell Death and Differentaition*, 8(4), pp.345–356.

Willis, S., Fletcher, J. & Kaufmann, T., 2007. Apoptosis initiated when BH3 ligands engage multiple Bcl-2 homologs, not Bax or Bak. *Science*, 315(5813), pp.856–859.

Willis, S.N. et al., 2005. Proapoptotic Bak is sequestered by Mcl-1 and Bcl-xL, but not Bcl-2, until displaced by BH3-only proteins. *Genes and Development*, 19(11), pp.1294–1305.

Wilson, A.M. et al., 2013. ASPP1/2 regulate p53-dependent death of retinal ganglion cells through PUMA and Fas/CD95 activation in vivo. *The Journal of Neuroscience : the Official Journal of the Society for Neuroscience*, 33(5), pp.2205–16.

Yamamoto, Y. & Henderson, C., 1999. Patterns of programmed cell death in populations of developing spinal motoneurons in chicken, mouse, and rat. *Developmental Biology*, 71(214), pp.60–71.

Youle, R.J. & Strasser, A., 2008. The BCL-2 protein family: opposing activities that mediate cell death. *Nature Reviews. Molecular Cell Biology*, 9(1), pp.47–59.

Zamorano, S. et al., 2012. A BAX/BAK and cyclophilin D-independent intrinsic apoptosis pathway. *PloS One*, 7(6), p.e37782.

Zheng, L. et al., 2006. Loss of BCL-XL in rod photoreceptors: Increased susceptibility to bright light stress. *Investigative Ophthalmology and Visual Science*, 47(12), pp.5583–5589.

Zhong, Q. et al., 2005. Mule/ARF-BP1, a BH3-only E3 ubiquitin ligase, catalyzes the polyubiquitination of Mcl-1 and regulates apoptosis. *Cell*, 121(7), pp.1085–95.

6.0 Appendix 1

Example calculation of the probability of collecting embryos of all genotypes.

Cross:	♀ **NesCre$^{+/-}$ Bcl-x$^{+/-}$**	**X**	♂ **Bcl-x$^{-/-}$**
Probability	*Genotype*		*Phenotype*
25%	NesCre$^{+/-}$ Bcl-x$^{-/-}$		BKO
25%	NesCre$^{+/-}$ Bcl-x$^{+/-}$		Bcl-x Het
25%	Bcl-x$^{-/-}$		Ctl (Not used)
25%	Bcl-x$^{+/-}$		Ctl

Cross:	♀ **Mcl-1$^{-/-}$**	**X**	♂ **NesCre$^{+/-}$ Mcl-1$^{+/-}$**
Probability	*Genotype*		*Phenotype*
25%	NesCre$^{+/-}$ Mcl-1$^{-/-}$		MKO
25%	NesCre$^{+/-}$ Mcl-1$^{+/-}$		Mcl-1 Het
25%	Mcl-1$^{-/-}$		Ctl (Not used)
25%	Mcl-1$^{+/-}$		Ctl

Cross:	♀ **NesCre$^{+/-}$ Mcl-1$^{+/-}$ Bcl-x$^{+/-}$**	**X**	♂ **Mcl-1$^{+/-}$ Bcl-x$^{-/-}$**
Probability	*Genotype*		*Phenotype*
6.25%	NesCre$^{+/-}$ Mcl-1$^{-/-}$ Bcl-x$^{-/-}$		DKO
6.25%	NesCre$^{+/-}$ Mcl-1$^{-/-}$ Bcl-x$^{+/-}$		MKO: Bcl-x Het
12.5%	NesCre$^{+/-}$ Mcl-1$^{+/-}$ Bcl-x$^{-/-}$		Mcl-1 Het: BKO
6.25%	NesCre$^{+/-}$ Mcl-1$^{+/+}$ Bcl-x$^{-/-}$		BKO
12.5%	NesCre$^{+/-}$ Mcl-1$^{+/-}$ Bcl-x$^{+/-}$		Mcl-1 Het: Bcl-x Het
6.25%	NesCre$^{+/-}$ Mcl-1$^{+/+}$ Bcl-x$^{+/-}$		Bcl-x Het
6.25%	Mcl-1$^{-/-}$ Bcl-x$^{-/-}$		Ctl (Not used)
6.25%	Mcl-1$^{-/-}$ Bcl-x$^{+/-}$		Ctl (Not used)
12.5%	Mcl-1$^{+/-}$ Bcl-x$^{-/-}$		Ctl (Not used)
6.25%	Mcl-1$^{+/+}$ Bcl-x$^{-/-}$		Ctl (Not used)
12.5%	Mcl-1$^{+/-}$ Bcl-x$^{-+/-}$		Ctl
6.25%	Mcl-1$^{+/+}$ Bcl-x$^{+/-}$		Ctl

Presence of Cre allele indictaed by +/-.

For Mcl-1 and Bcl-x: + = wild type allele, - = floxed allele.

7.0 Appendix 2

Example relative quantity (RQ) calculation for expression level of Mcl-1. Ct= threshold cycle, Ct_m= mean Ct,

1. $Ct_m = (Ct_1 + Ct_2 + Ct_3) / 3$

Sample Name	Target Name	C_T	CT_m
Sample1	Mcl-1	24.90413	24.9391
Sample1	Mcl-1	24.95422	
Sample1	Mcl-1	24.95894	
Sample2	Mcl-1	24.9531	24.83001
Sample2	Mcl-1	24.67272	
Sample2	Mcl-1	24.86421	
Ctl	Mcl-1	24.62112	24.61618
Ctl	Mcl-1	24.59992	
Ctl	Mcl-1	24.62749	
Sample1	Gapdh	17.62559	17.67149
Sample1	Gapdh	17.69476	
Sample1	Gapdh	17.6941	
Sample2	Gapdh	17.53425	17.56478
Sample2	Gapdh	17.53213	
Sample2	Gapdh	17.62796	
Ctl	Gapdh	18.78459	19.07336
Ctl	Gapdh	19.24463	
Ctl	Gapdh	19.19085	

2. $\Delta Ct = Ct_{m1} - Ct_{mGAPDH}$

Sample Name	CT_{mMcl-1}	CT_{mGAPDH}	ΔCt
Sample1	24.9391	17.67149	7.267612
Sample2	24.83001	17.56478	7.26523
Ctl	24.61618	19.07336	5.542819

3. $\Delta\Delta Ct = \Delta Ct_1 - \Delta Ct_{Ctl}$

Sample Name	ΔCt_1	ΔCt_{Ctl}	$\Delta\Delta Ct$
Sample1	7.267612	5.542819	1.72479
Sample2	7.26523	5.542819	1.72241
Ctl	5.542819	5.542819	0

4. $RQ = 1 / 2^{(\Delta\Delta Ct)}$

Sample Name	$\Delta\Delta Ct$	RQ
Sample1	1.72479	0.30254
Sample2	1.72241	0.30304
Ctl	0	1